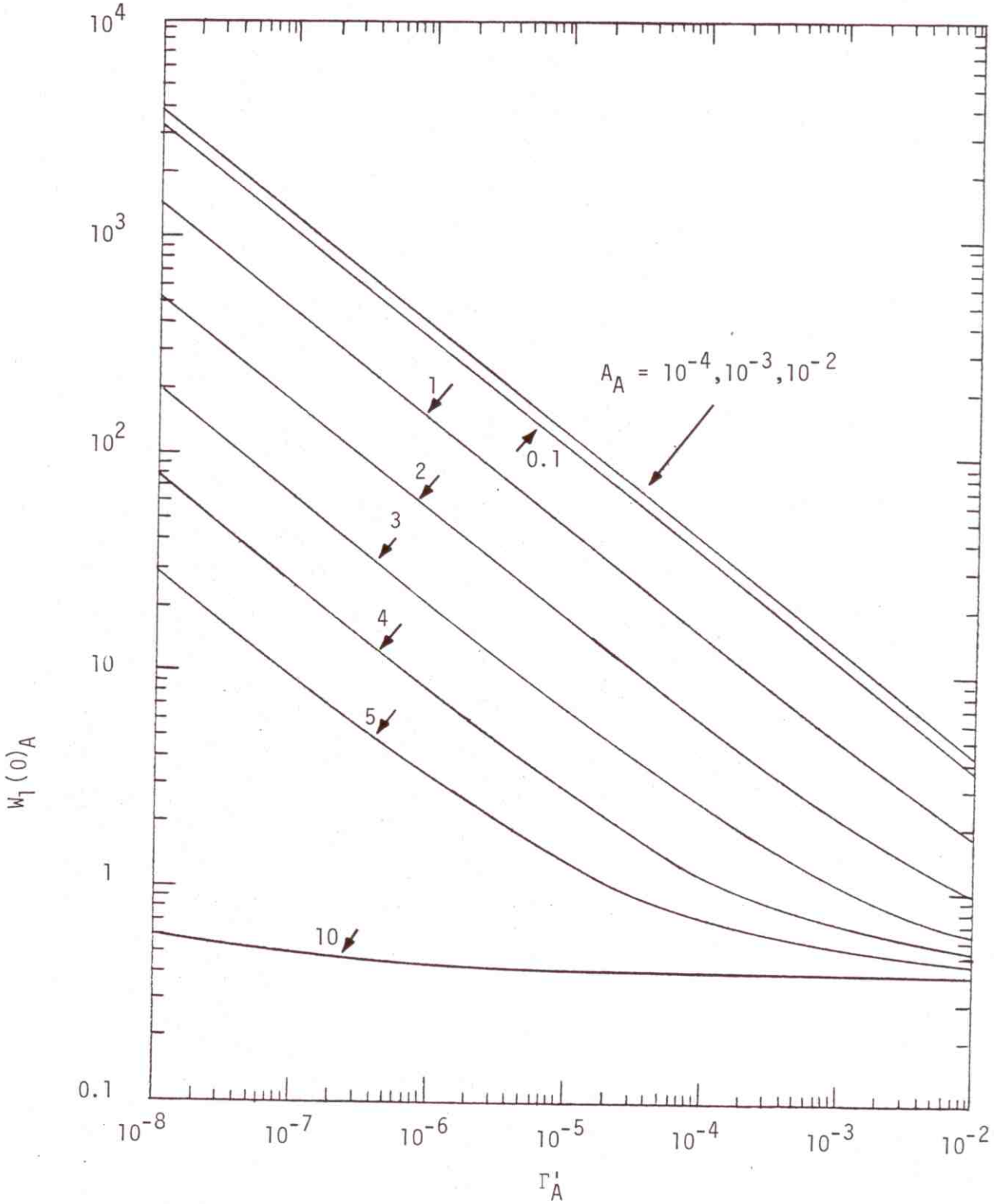

Figure 7.25. The probability density function, evaluated at zero, for Class A noise, Equation (7.35a).

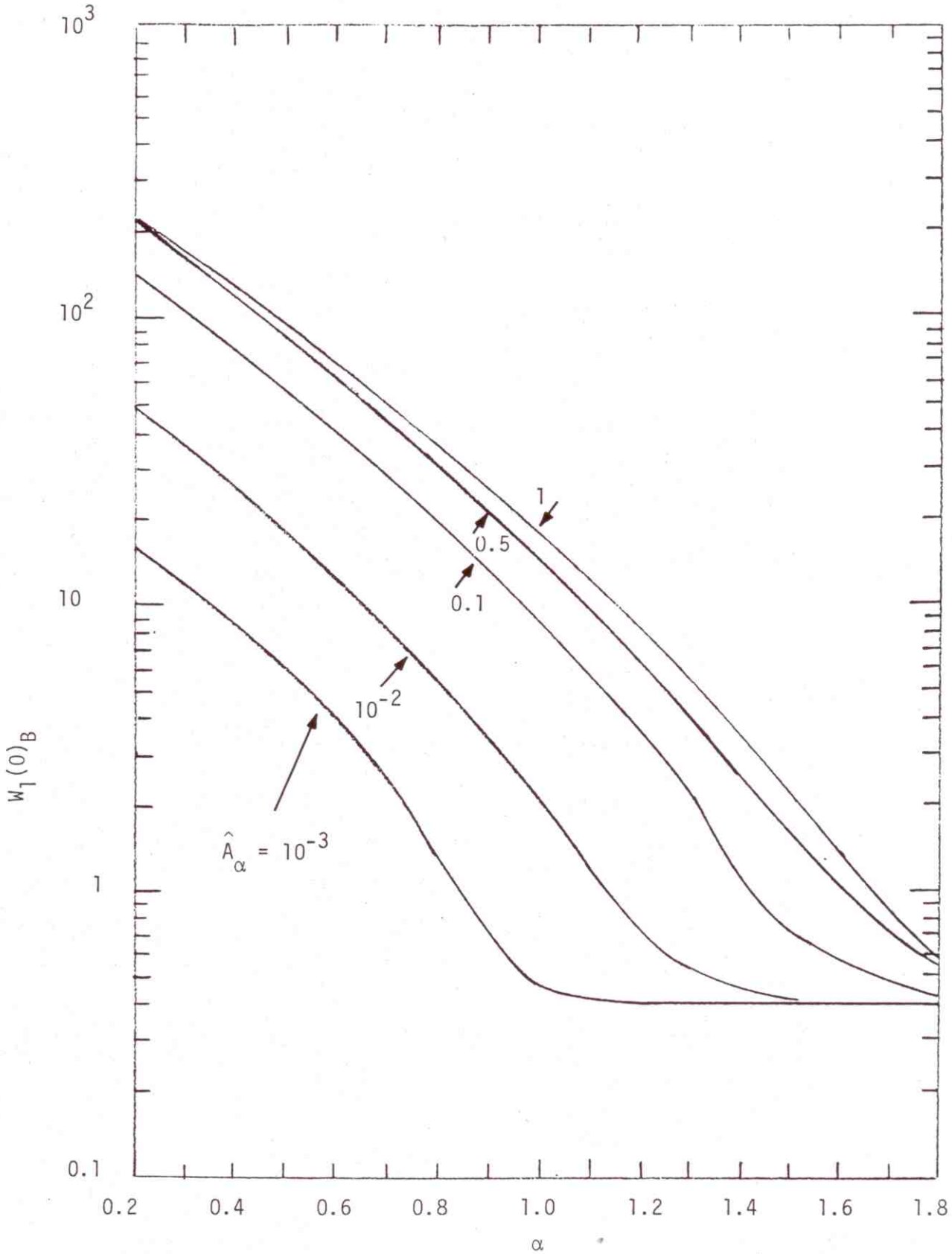

Figure 7.26. The probability density function, evaluated at zero, for Class B noise, Eq. (7.36).

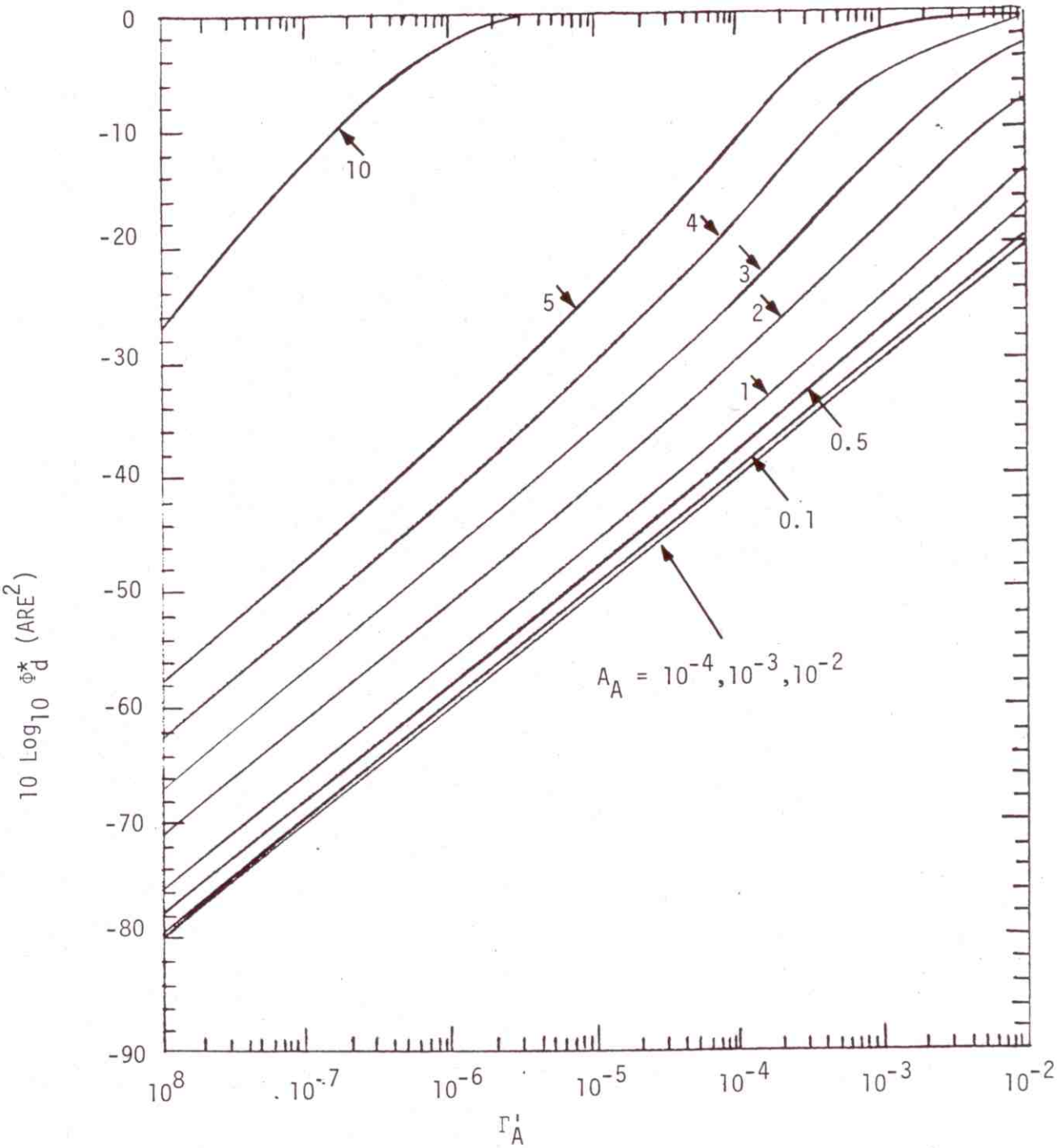

Figure 7.27. The square of the asymptotic relative efficiency, $ARE^2(\Phi_d^*)$, of the simple correlator versus the locally optimum detector for coherent reception, (1) of Table 7.1, for Class A noise.

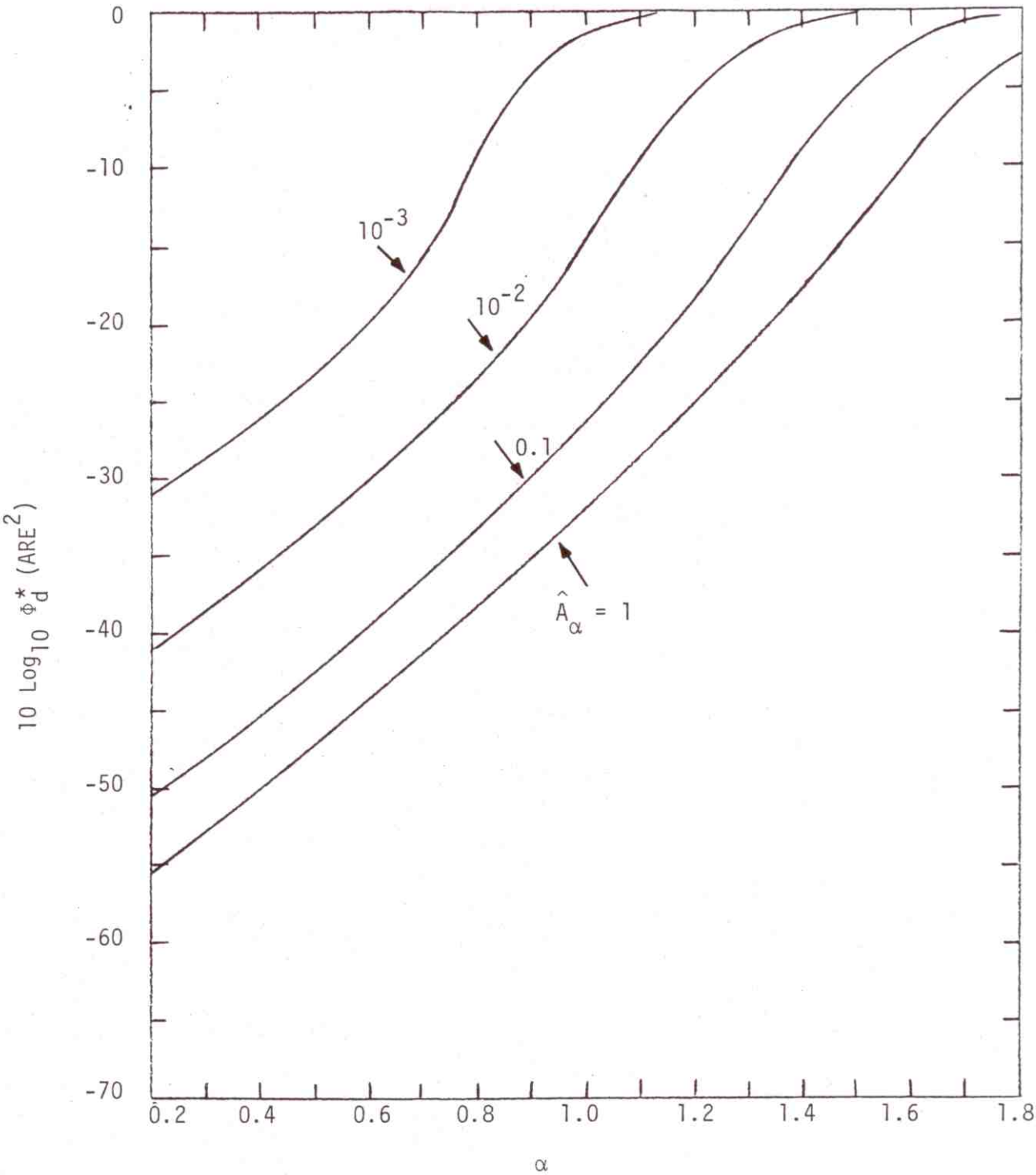

Figure 7.28. The square of the asymptotic relative efficiency, $ARE^2_{\cdot}(\Phi_d^*)$, of the simple correlator versus the locally optimum detector for coherent reception, (1) of Table 7.1, for Class B noise.

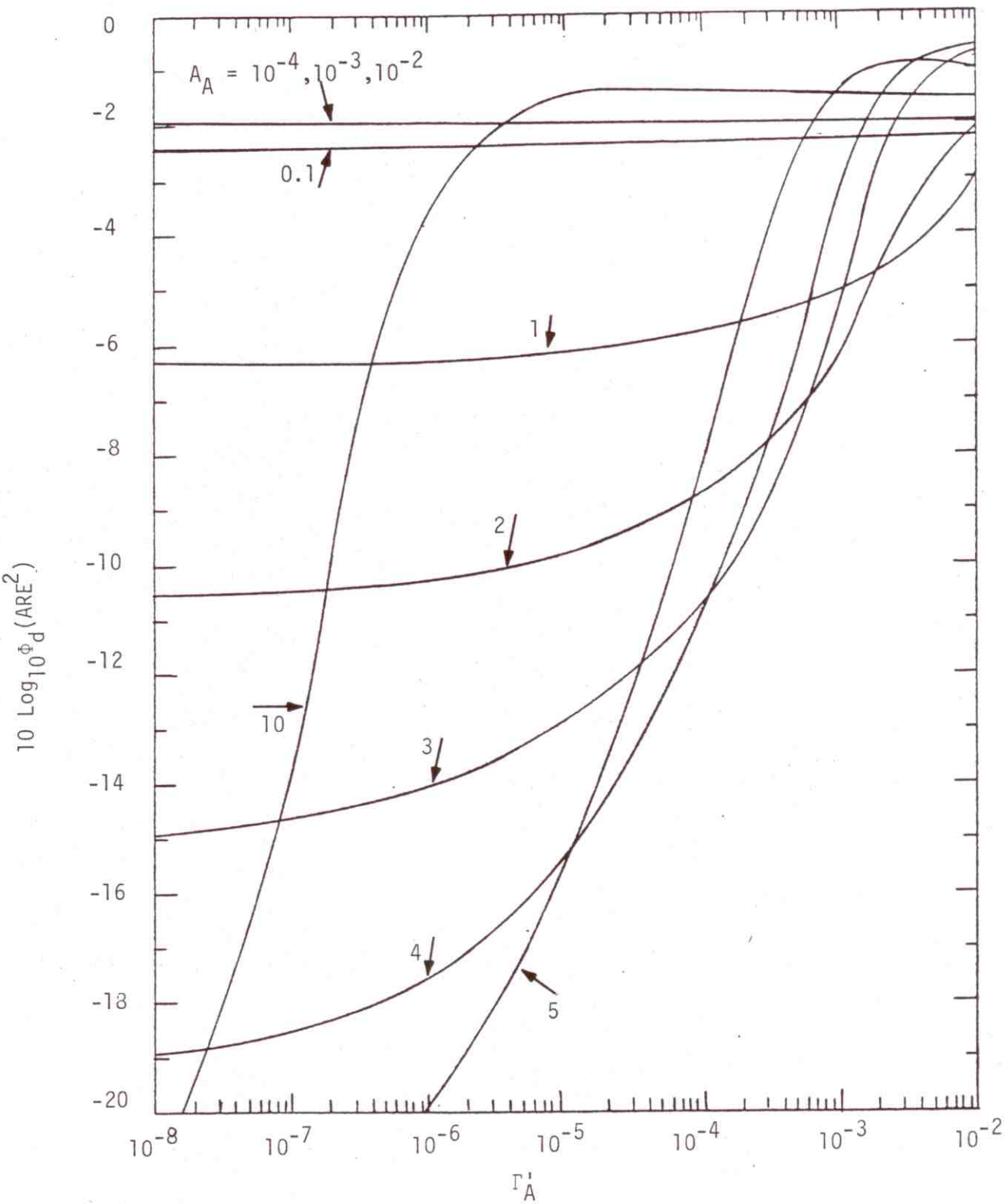

Figure 7.29. The square of the asymptotic relative efficiency, $ARE^2 \ (\Phi^*_d)$, of the clipper correlator (hard limiter) versus the locally optimum detector for coherent reception, (2) of Table 7.1, for Class A noise.

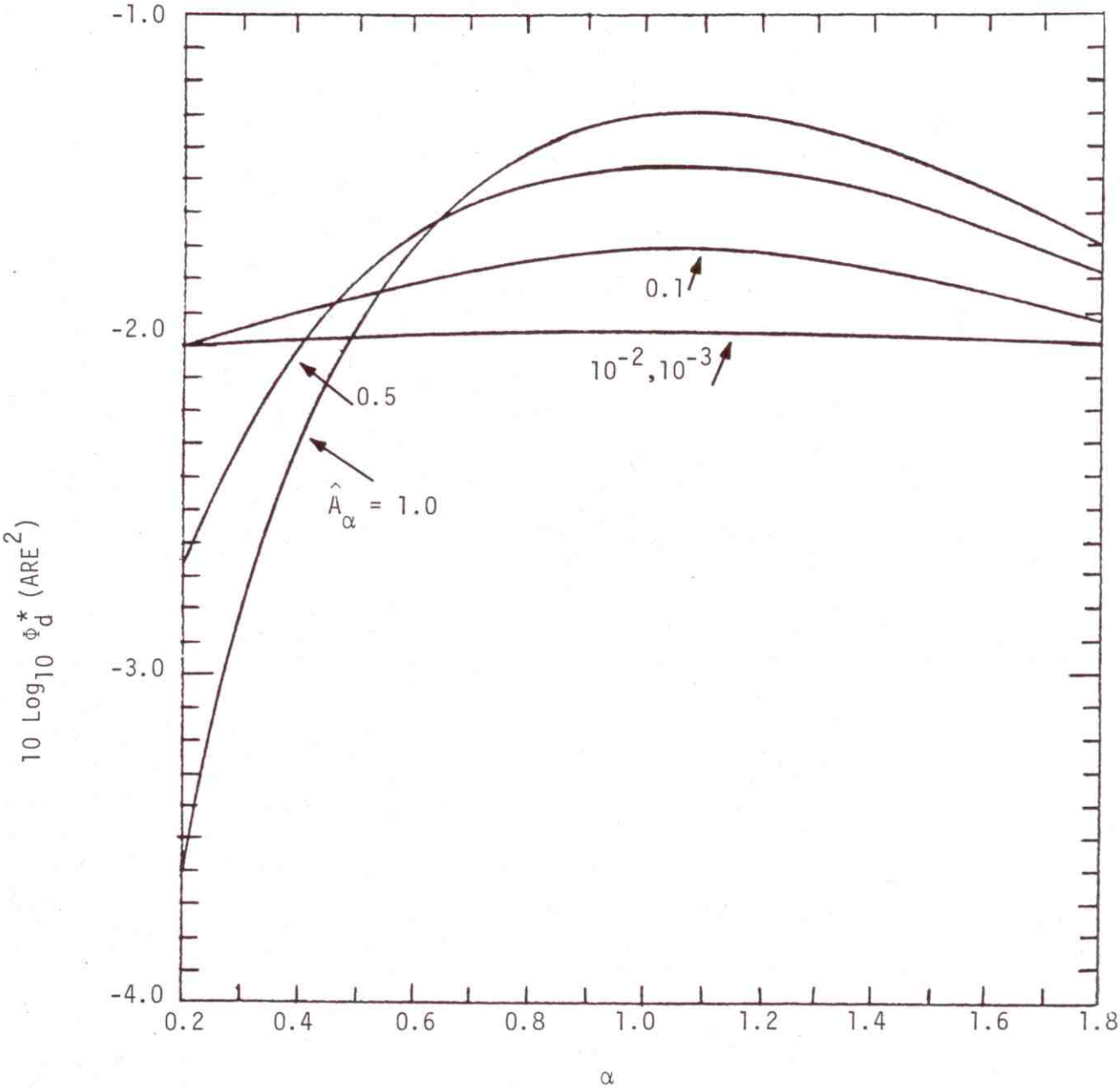

Figure 7.30. The square of the asymptotic relative efficiency, $ARE^{*}(\Phi_d^*)$, of the clipper correlator (hard limiter) versus the locally optimum detector for coherent reception, (2) of Table 7.1, for Class B noise.

7.5 Brief Remarks on Figures 7.1-7.30:

Figures 7.1, 7.2 show the (zero-memory) dynamic characteristics of the LOBD's for several specific Class A and Class B noise cases. Both Class A and B noise require a combination of linear amplifier, and clipper-suppression (negative gain) for the larger amplitudes. The Class A characteristics are, however, somewhat more complex, with a second amplifying-limiting region, cf. Figure 7.1 vs. 7.2. In the Class B cases the characteristic is a clipper-suppressor which is rather insensitive to the nongaussian nature ($\sim\hat{A}_\alpha$) and to the source distribution and propagation conditions ($\sim\alpha$) of the noise.

Figures 7.3-7.6 are essentially self-explanatory: increasing variances (σ_o^{*2}) lead to smaller error probabilities and larger probabilities of correct signal detection, with smaller false alarm probabilities (α_F^*) requiring larger σ_o^{*2}, all of which is entirely expected. Similarly, the tighter the controls the better the performance, as shown in Figures 7.5, 7.6.

In Figures 7.7-7.10 all these Class A nongaussian noise statistics $L_A^{(2)}$, $L_A^{(4)}$, etc., approach their respective limiting gaussian values as $A_A\to\infty$, as expected ($\Gamma_A'>0$); i.e., $L_A^{(2)}\to 1$, $L_A^{(4)}\to 2$, $L_A^{(2,2)}\to 6$, $L_A^{(6)}\to 8$, cf. (7.16). Moreover, when $A_A\to 0$, $\Gamma_A'\to 0$, we also obtain the gaussian limits, as expected, due to the nonvanishing gaussian component $\sigma_G^2>0$ (i.e., $\Gamma_A'\to\infty$). And, of course, the more highly nongaussian is the noise $A_A \doteq \varepsilon(>0)$ the larger is the magnitude of the statistic in question.

The behavior of the corresponding Class B statistics (Figures 7.11-7.24) is similar, although plotted differently. For $\hat{A}_\alpha(\sim A_B)\to\infty$, the curves for $L_B^{(2)}$ etc., fold back on each other, approaching zero db for $L_B^{(2)}\to 1$, 3 db for $L_B^{(4)}\to 2$, etc., cf. (7.16). Similarly, as $\hat{A}_\alpha\to 0$ (i.e., $A_B\to 0$) with $\sigma_{\hat{G}}^2>0$, one again has a gaussian pdf, cf. (7.11a), which becomes $w_1(\hat{x})_G=e^{-\hat{x}^2}/\sqrt{\pi}$, as expected, with $\hat{x}\to X/\sigma_G\sqrt{\Omega_B}$, (7.10). Smaller values of α represent more effectively nongaussian interference; i.e., larger values of $L_B^{(2)}$, etc., consistent with the more radical departures of the pdf form gaussian behavior as $|\hat{x}|\to\infty$ [cf. Figure 3.4(II) of [6], for the APD P_{1B} $(\varepsilon\geq\varepsilon_o)$].

The processing gains (per independent sample), as shown in Figures 7.15,7.16, for signals with partially incoherent structure ($Q_n=10$, $n\gg 1$) show the same type of behavior as the various nongaussian noise moments

$L_A^{(2)}$, $L_B^{(2)}$, etc., in Figures 7.7-7.14, and for the same reasons. [For coherent threshold reception, see Figures 7.7,7.11.]

Figures 7.17-7.22 show various bounding values for minimum detectable signals under the equal variance condition (I), Sec. 6.4, for coherent and incoherent reception; see also Figure 6.1 and the discussion of III, Sec. 6.4 above. In general, as the noise becomes more gaussian, these bounds become looser, and vice versa as the interference becomes more nongaussian; e.g., A_A, $\hat{A}_\alpha$, Γ'_A, α, etc. This is consistent with our general observation that the more nongaussian the noise, the smaller, i.e., the tighter the upper bound on the maximum minimum detectable signal $\left\langle a_o^2 \right\rangle^*_{min}$ permitted under the A0 or equal variance condition.

Figures 7.23a-7.24 compare suboptimum performance against the corresponding optimum performance measures, with the degradation factor, Φ_d^*, as parameter. These curves are entirely canonical in that they apply for any nongaussian (and gaussian) noise, common mode of reception (i.e., coherent, incoherent, or composite), cf. (6.48), and (6.84) vs. (6.90), as long as sample size (n) is large and the A0 condition (equal-variance conditions) is obeyed. Thus, once Φ_d^* is properly determined, specific performance measures are at once obtained from these figures.

Figures 7.25,7.26 show typical pdf's at x=o for Class A and B noise, needed in the calculation of the performance of clipper-correlators and comparisons with other optimum and suboptimum threshold detection algorithms, cf. Table 7.1 above.

Finally, Figures 7.27-7.30 show typical Asymptotic Relative Efficiencies[2] (ARE's)[2], viz. Φ_d^*'s, of suboptimum detectors vs. the optimum for the noise in question and the particular mode of observation, in these threshold situations, discussed throughout this study. Characteristically, since the simple correlator is optimum in gaussian noise, as the noise becomes more gaussian, the ARE's for the simple correlator in both Class A and B noise becomes larger (i.e., closer to unity), cf. Figures 7.27,7.28, including $\alpha \to 2$ in the latter (i.e., larger α means less nongaussian, with a fold-over effect in Class B noise as $\hat{A}_\alpha \to \infty$ (not shown in the figures). The ARE's for the clipper-correlator, however, display a fold-over effect as the noise

becomes more nongaussian, until for small A_A, $O(\leq 10^{-1})$, close to the maximum value (0 db) is attained. This maximum cannot be reached here, of course, since the clipper-correlator is never optimum in Class A as gauss noise, although the difference is small, viz., $\frac{2}{\pi} = -2$ db, cf. Eq. (6.66). A similar behavior is also noted for the clipper-correlator in Class B noise, cf. Figure 7.30, although the range of the fold-over effect as the noise goes from very nongaussian to gauss is much smaller, on the scale of a 10th the amount of the corresponding Class A effect. This shows that the super-clipper (i.e., clipper-correlator) is much less sensitive to impulsive noise (Class B) than to the "coherent" (Class A) noise. Thus, the clipper-correlator makes a comparatively robust processor against Class B noise, and can be fairly close O(4 db to 1.5 db) to the optimum processor in performance, cf. Figure 7.30.

7.6 Numerical Examples (Threshold Detection):

In this (sub) Section, we present a few numerical examples to illustrate the use of the general results of the preceding text. Typical Class A and B noise parameters and scenarios are selected; our attention here is given mainly to the on-off-cases, for comparative simplicity. Thus, we have

$$\underline{\text{Class A Interference}}: \quad A_A = 0.35; \ \Gamma_A' = 5 \times 10^{-5} \quad \text{(canonical, [9])} \tag{7.39a}$$

$$\underline{\text{Class B Interference}}: \quad \hat{A}_\alpha = 1.0; \ \alpha = 1.2; \ \Omega = 0.00207, \quad \text{("Saipan Noise," [33])}^\dagger \tag{7.39b}$$

with the various other parameters of observation being $n = 10^4$, $p_D^* = 0.90$, $P_e^* = 10^{-4}$, $\alpha_F^* = 10^{-4}$, typically; symmetrical channels are also assumed: $p = q = 1/2$, $\gamma_{I.0} = 1$. Typical results follow below.

---

†The value of $L^{(2)}$ in [33] is 4.5 db higher as a result of different intensity normalization and scaling.

I. Optimum Detection

Example 1: Performance Probabilities:

From Figures 7.3,7.4 we find at once for the values of P_D^*, P_e^*, α_F^* above that

$$\sigma_o^{*2}\Big|_{I.O} = 17.3 \text{ db } (p_e^* = 10^{-4}); \quad \sigma_o^{*2}\Big|_{N.P.} = 14.2 \text{ db} \qquad (7.40)$$

$$(\alpha_F^* = 10^{-4},\ p_D^* = 0.9);\ n>>1 \quad .$$

These results apply directly, also, to suboptimum detectors (σ_o^2, etc.), for values of $P_e = P_e^*$, etc., again, provided the sample size is large ($n>>1$) and that $\sigma_1^2 \doteq \sigma_o^2$: the equal variance condition holds (so that Eq. (7.13) remains valid).

Related to the above are the results of Figures 7.5,7.6, for $\sqrt{B^*} = C^*$, etc. For the performance measures of our example above, we find at once that

$$\sqrt{B^*} = C_{N.P.}^* = 5.6 \text{ db } (= 3.63)\ ;\ C_{I.O}^* = 7.2 \text{ db } (= 5.25) \qquad (7.41)$$

Example 2: Coherent Detection in Class A Noise:

Here we wish to establish the minimum detectable signal $\left\langle a_o^2 \right\rangle_{\text{min-coh}}^*$ associated with the above operating conditions when the Class A noise of (7.39a) above embodies the interference. From (6.10) in (6.11a,b) we get directly

$$\boxed{\left\langle a_o^* \right\rangle_{\text{min-coh}}^2 = \frac{B^*}{nL_A^{(2)}\,(1-\eta)}} \quad ; \quad (1-\eta \equiv \overline{a}_o^2 \Big/ \overline{a_o^2}\ ;\ 0 \le \eta < 1). \qquad (7.42)$$

For no or shallow fading, i.e., $\eta \sim 0$, but complete signal coherence ($\overline{s}_i = \sqrt{2}$), the upper bound, $x_{max} << x_{OA}^*$ on the permitted values of minimum detectable signal which still preserve the AO character of this optimum threshold algorithm is given by (6.71)

$$\overset{v}{x}_{max} = \overset{v}{x}^{*}_{0A} - 15 \text{ db} \quad ; \quad \overset{v}{x}^{*}_{0A} = 10 \log 3 \times 10^{-5} = -45 \text{ db (Fig.7.17)}, \tag{7.43}$$

so that the upper bound here is $\overset{v}{x}_{max} = -45-15 = -60$ db. [The "<<" in $x_{max} << x^{*}_{0A}$ is usually taken to be 15 db.]

Next we use (7.42), $\overset{v}{n} = 40$ db, with $L_A^{(2)} = 41.5$ db from Figure 7.7 and $B^* = 11.2$ db for the N.P. detector from (7.41), so that

$$\left\langle \overset{v}{a}_o^2 \right\rangle^{*}_{min\text{-}coh} \Big|_{N.P.} = 11.2 - 40 - 41.5 = -70.3 \text{ db}, \tag{7.44a}$$

which is substantially below the x_{max} bound (-60 db), so that the AO condition is amply satisfied. Likewise, from (7.41) for the I.O. we obtain

$$\left\langle \overset{v}{a}_o^2 \right\rangle^{*}_{min\text{-}coh} \Big|_{I.O.} = 14.4 - 40 - 41.5 = -67.1 \text{ db}. \tag{7.44b}$$

If the fading is moderately deep, e.g., $\eta = 0.99$, $(1\overset{v}{-}\eta) = -20$ db, then the x^{*}_{0A} obtained from (6.71) using $L^{(2)}$ and $L^{(2,2)}$ from Figures 7.7 and 7.9, $L^{(2)} = 41.5$ db, $L^{(2,2)} = 90$ db, is $x^{*}_{0A} = 2.8 \times 10^{-5}$ or $\overset{v}{x}_{max} = -45.5-15 = -60.5$ db. Again from (7.41) and (7.42), with $(1\overset{v}{-}\eta) = -20$ db, we obtain

$$\left\langle \overset{v}{a}_o^2 \right\rangle^{*}_{min\text{-}coh} \Big|_{N.P.} = 11.2-40-41.5+20 = -50.3 \text{ db},$$

and

$$\left\langle \overset{v}{a}_o^2 \right\rangle^{*}_{min\text{-}coh} \Big|_{I.O.} = 14.4-40-41.5+20 = -47.1 \text{ db}, \tag{7.44c}$$

which are above the x_{max} bound, so that the estimate of $\left\langle a_o^2 \right\rangle^{*}_{min}$ may be suspect.

Example 3: Coherent Detection in Class B Noise:

For this example we repeat the calculations of $\left\langle a_o^2 \right\rangle^{*}_{min\text{-}coh}$, (7.42), in the manner of Example 2, but now with the values of $L_B^{(2)}$, $\overset{v}{x}^{*}_{o}$ appropriate to our particular Class B case (7.39b). From Figures 7.11 and

7.13 we get $L_B^{(2)} = 25$ db and $L_B^{(2,2)} = 56$ db. For no or shallow fading ($\eta = 0$), $\overset{v}{x}{}_o^* = -25$ db (Figure 7.20), and for moderate or deep fading ($\eta \geq 0.99$), $\overset{v}{x}{}_o^* = -28.2$ db. From (7.41) in (7.42), with $n = 10^4$, we obtain, for no or little fading

$$\left\langle a_o^2 \right\rangle^*_{\text{min-coh}} \Big|_{\text{N.P.}} = 11.2\text{-}40\text{-}25 = -53.8 \text{ db}, \tag{7.45a}$$

$$\left\langle a_o^2 \right\rangle^*_{\text{min-coh}} \Big|_{\text{I.O.}} = 14.4\text{-}40\text{-}25 = -50.6 \text{ db}, \tag{7.45b}$$

with $\overset{v}{x}{}_{max} = -25\text{-}15 = -40$ db. With even moderately deep fading [O(20db)], $\overset{v}{x}{}_{max} = -43.2$ db and $a_o^{2\,*}{}_{\text{min-coh}} = -33.8$ db and -30.6 db, respectively, for N.P. and I.O., so that even moderate fading cannot be tolerated.

Example 4: Incoherent Detection in Class A Noise:

We parallel Example 2, for the conditions as before, but now using (6.24) and (6.25) in (6.27), or (7.19a) with (7.20a) above in conjunction with (6.27), to write for the minimum detectable signal in Class A noise, when threshold detection is incoherent:

$$\left\langle a_o \right\rangle^*_{\text{min-inc}} = \left\{ 8\, B^* \Big/ nL^{(4)} \left[1 + \frac{2L^{(2)^2}}{L^{(4)}} (Q_n - 1) \right] \right\}^{\frac{1}{2}} \tag{7.46}$$

Now, from (6.58)' we have for coherent sinusoidal waveforms

$$Q_n \doteq \frac{n}{2} \text{ (slow fading)} \; ; \; Q_n \doteq \frac{n}{2} (1-\eta)^2 \text{ (rapid fading)}. \tag{7.46a}$$

For incoherent signal waveforms, $Q_n - 1 \doteq 0$. Accordingly, for the large samples ($n \gg 1$) required for (AO) threshold detection, (7.46) reduces to

(i) coherent signals:

$$\left\langle a_o^2 \right\rangle^*_{\text{min-inc}} \Big|_{\text{slow}} = \sqrt{8B^*}/nL^{(2)} \ ,$$

and (7.47a)

$$\left\langle a_o^2 \right\rangle^*_{\text{min-inc}} \Big|_{\text{rapid}} = \sqrt{8B^*}/nL^{(2)}(1-\eta), \ \frac{n}{2}(1-\eta)^2 >> 1 \ ,$$

since $L^{(2)^2}/L^{(4)} = O(1)$. (In fact, from Figures 7.7 and 7.8, $L^{(2)} = 41.5$ db, $L_A^{(4)} = 86$ db, so that $L^{(2)^2}/L^{(4)} = -3$ db.)

With incoherent signal structure ($Q_n = 1$), (6.46) reduces, for both slow and rapid fading, to

(ii) incoherent signals:

$$\left\langle a_o^2 \right\rangle_{\text{min/inc}} \doteq \sqrt{8B^*/nL^{(4)}} \ . \tag{7.47b}$$

Specific numerical results may be obtained at once for the postulated observation conditions above. We have [cf. (7.41)]:

$$\left\langle a_o^2 \right\rangle^*_{\text{min-inc}} \Big|_{\substack{\text{coh.sig.} \\ \text{slow} \\ \text{N.P.}}} = 4.5+5.6-40-41.5 = -71.4 \text{ db}, \tag{7.48a}$$

$$\left\langle a_o^2 \right\rangle^*_{\text{min-inc}} \Big|_{\substack{\text{coh.sig.} \\ \text{rapid} \\ \text{N.P.}}} = -71.4-(1\overset{v}{-}\eta) \text{ db}, \quad \text{and} \tag{7.48b}$$

$$\left\langle a_o^2 \right\rangle^*_{\text{min-inc}} \Big|_{\substack{\text{inc.sig.} \\ \text{any} \\ \text{N.P.}}} = 4.5+5.6-20-43 = -52.4 \text{ db} \ . \tag{7.48c}$$

The corresponding results for the I.O. are 1.6 db greater (=7.2-5.6) from (7.41). As expected, incoherent signal waveforms result in truly incoherent

detection, with a $\sqrt{n}$ -dependence on sample size vs. the n-dependence obtainable with coherent waveforms. Thus, a channel which destroys signal coherence greatly reduces the detectability of the resultant signal (O(20 db) here), as is well-known.

To complete our analysis, we need to establish the bound $y_{max} << y_o^*$. From Figure 7.19 for coherent waveforms, and Figure 7.18 for the incoherent waveform cases, we get respectively for y_o^*,

$$y_{OA}^* \Big|_{\text{coh-sig}} = -52.5 \text{ db} \; ; \; y_{OA}^* \Big|_{\text{inc-sig}} = -54 \text{ db} \; . \tag{7.49}$$

Our results (7.48a,c) above for the coherent signals fall acceptable below $y_{max} = -52.5\text{-}15 = -67.5$ db, as long as the rapid fading is not too deep, but for the incoherent signals sample-size is not sufficiently large to put $\langle a_o^* \rangle^*_{\text{min-inc}}$ below y_o^* to insure the AO character of the algorithm (and that the performance measures are themselves the required good approximations). Thus, this last result, (7.48c), really represents a suboptimum threshold algorithm, with a suspect estimate of $\langle a_o^2 \rangle_{min}$, and performance.

Finally we note the "anomalous" behavior here of (optimum) coherent versus incoherent detection: $\langle a_o^2 \rangle^*_{\text{min-coh}} > \langle a_o^2 \rangle^*_{\text{min-inc}}$ for otherwise the same reception conditions[†]. For a discussion of this effect, see Section 6.4,III and Figure 6.1.

[†] We note that the "anomalies" are not due to the particular values of $L^{(2)}_{A,B}$, but rather reside analytically in the quantities $B^*_{N.P.}$ or $B^*_{I.O.}$; i.e., from (7.42) and (7.47a),

$$\langle a_o^2 \rangle^*_{\text{min-coh}} - \langle a_o^2 \rangle^*_{\text{min-inc}} = (B^* - \sqrt{8B^*})/nL^{(2)}(1-\eta) \; .$$

From Figures 7.5 and 7.6 we see that $B^* - \sqrt{8B^*} < 0$, i.e., $\langle a_o^2 \rangle^*_{\text{min-coh}} < \langle a_o^2 \rangle^*_{\text{min-inc}}$, for those P_e^* or p_D^* where $C^* = \sqrt{B^*} < \sqrt{8} = 4.5$ db, i.e., when $P_e^* > 2 \times 10^{-2}$, or when $p_D^* < 0.62 (\alpha_F^* = 10^{-4})$. Physically, as discussed in Section 6.4, III, this "anomalous" behavior stems from the different amounts of signal and noise information lost and gained for incoherent vis-à-vis coherent detection.

Example 5: Incoherent Detection in Class B Noise:

The analytic results (7.47) apply equally well here, with now $L_B^{(2)} = 25$ db and $L_B^{(4)} = 53.5$ db from Figure 7.12. From Figures 7.21,7.22 we get the limits

$$y_{0B}^* = -35.5 \text{ db (inc.sig.)} \; ; \; y_{0B}^* = -36.6 \text{ db (coh. sig.)} \; . \qquad (7.50)$$

We summarize the results for the corresponding minimum detectable signals:

$$\begin{aligned} \langle a_o^2 \rangle^* &= -54.9 \text{ db} && \text{(coh.sig.,slow,N.P.),} \\ &= -54.9 - (1 \overset{v}{-} \eta) \text{ db} && \text{(coh.sig.,rapid,N.P.),} \\ &= -36.1 \text{ db} && \text{(inc.sig.,any,N.P.),} \end{aligned} \qquad (7.50a)$$

again with the I.O. results 1.6 db greater. With $y_{max} \ll y_{0B}^*$, or $y_{max} = -50.5$ db for coherent signal structures, the minimum detectable is acceptably below y_{max}. On the other hand, larger sample sizes are needed to make the minimum detectable signals fall within acceptable AO limits when the signal waveform is incoherent.

Example 6: Composite Detection in Class A and B Noise:

From the results of Section 6.5 (6.88a,b) we may write for the minimum detectable signal when an (optimum) composite threshold detection is used, the following special results for coherent signal waveforms:

$$\langle a_o^2 \rangle^*_{\text{min-comp}} \Big|_{\text{slow}} \doteq \frac{\sqrt{8B^*} - 4\,(1-\eta)}{nL^{(2)}} \; , \quad B^* \gg 2(1-\eta)^2 \; , \qquad (7.51a)$$

$$\langle a_o^2 \rangle^*_{\text{min-comp}} \Big|_{\text{rapid}} \doteq \frac{\sqrt{8B^*} - 4}{nL^{(2)}(1-\eta)} \; , \; B^* \gg 2, \; Q_n \gg 1 \; . \qquad (7.51b)$$

[For incoherent signal waveforms ($\Pi_{coh}^* \to 0$), the composite detector, of course, reduces to the purely incoherent detector of (7.47a), discussed in Examples 4,5 above.]

Comparing (7.51a,b) with (7.47a) we see that $\langle a_o^2 \rangle^*_{\text{min-comp}} < \langle a_o^2 \rangle^*_{\text{min-inc}}$ always for slow or rapid fading: there is no "anomalous" behavior here. Moreover, it is easy to demonstrate this; for example, let $x=B^*$, so that (7.51a) vs. (7.47a) becomes

$$\begin{aligned} \sqrt{8x}-4(1-\eta) &\overset{?}{\leq} \frac{x}{1-\eta} \\ 0 &\leq \frac{x^2}{(1-\eta)^2} + 16(1-\eta)^2, \quad \text{all } x \geq 0 \ , \end{aligned} \tag{7.52}$$

and similarly for (7.51b).

One important feature of the composite (threshold) detector to be noted is its insensitivity to slow fading, vis-à-vis the coherent detector, i.e., (7.51a) vs. (7.42). A second is the possibly strong superiority over either the coherent or incoherent detector, as expressed by smaller minimum detectable signals, particularly when there is significant fading. This superiority vs. the incoherent detector is 0(1.5 db) and is 0 (3 db) vs. the coherent detector with no fading, as the numerical results below indicate, and is 0 (10-20 db) when there is moderate fading (η=0.99).

For the specific noise and signal examples assumed here we have for no fading:

$$\underline{\text{Class A}}: \quad \langle a_o^2 \rangle^*_{\text{min-comp}} = \frac{2.83 \times 3.63 - 4}{10^4 \times 1.41 \times 10^4} = -73.6 \text{ db} \quad \text{(N.P.)} \ , \tag{7.53a}$$

with the corresponding result for the I.O. of -71.1 db.

$$\begin{aligned} \underline{\text{Class B}}: \quad \langle a_o^2 \rangle^*_{\text{min-comp}} &= \frac{2.83 \times 3.63 - 4}{10^4 \times 3.16 \times 10^2} = -57 \text{ db} \quad \text{(N.P.)} \\ &= -54.7 \text{ db} \quad \text{(I.O.)} \ . \end{aligned} \tag{7.53b}$$

These figures are to be compared with (7.44a,b) and (7.45a) for the corresponding coherent detector results and with (7.48a) for the corresponding incoherent detector results.

For moderate slow fading (η=0.99), (7.51a) gives:

$$\underline{\text{Class A}}: \quad \left\langle a_o^2 \right\rangle^*_{\text{min-comp}} = \frac{2.83 \times 3.63 - 4(.01)}{10^4 \times 1.41 \times 10^4} = -71.4 \text{ db (N.P.)} \qquad (7.53c)$$

with the corresponding result for the I.O. of -69.8 db.

$$\underline{\text{Class B}}: \quad \left\langle a_o^2 \right\rangle^*_{\text{min-comp}} = \frac{2.83 \times 3.63 - 4(.01)}{10^4 \times 3.16 \times 10^2} = -54.9 \text{ db (N.P.)} \qquad (7.53d)$$

$$= -53.3 \text{ db (I.O.)} \ .$$

The corresponding fading results are given by (7.44c) for the coherent detector (Class A).

In general, the composite detector is to be recommended for its comparative insensitivity to slow fading. Observe that the stricter of the two possible bounds (x_o^*, y_o^*) is that for incoherent detection, i.e., from examples 2,3 and (7.49),(7.50) we have y_{OA}^* = -52.5 db (coh.sig. structure) and y_{OB}^* = -36.6 db, similarly. The results (7.53a,b) are accordingly within the limits $y_{\text{max-A}}$ = -52.5 - 15 = -67.5 db, and $y_{\text{max-B}}$ = -36.6 - 15 = -51.6 db.

Still other numerical examples can be readily constructed along these lines.

II. Suboptimum Detection and Comparisons:

Here let us use the results of Section 7.4, especially (7.25)-(7.38) and Table 7.1. We shall consider only a few examples here, by way of illustration.

For the two specific Class A and B noise cases, and reception conditions postulated here above, we begin by obtaining specific degradation factors (Φ_d^*) and ARE's from Figures 7.27-7.30 for coherent waveforms.

$$\underline{\text{Class A}}: \quad \Phi_d^* = -41.5 \text{ db} \quad \text{(Figure 7.27, simple correlator)}, \qquad (7.54)$$
$$\Phi_d^* = -\ 3.5 \text{ db} \quad \text{(Figure 7.29, clipper correlator)},$$

$$\underline{\text{Class B}}: \quad \Phi_d^* = -25.0 \text{ db} \quad \text{(Figure 7.28, simple correlator)}, \qquad (7.55)$$
$$\Phi_d^* = -\ 1.3 \text{ db} \quad \text{(Figure 7.30, clipper correlator)}.$$

Now, Φ_d^* measures the <u>increase</u> required for the (input) minimum detectable signal ($n>>1$) in suboptimum <u>coherent</u> threshold detection to obtain the same performance as the corresponding optimum threshold detector. Thus, we see that simple correlators are strongly degraded in Class A noise: 41.5 db in $\langle a_o^2 \rangle_{\text{min-coh}}$ for our particular example. On the other hand, the degradation is a much less severe, though a noticeable 3.5 db, when the suboptimum clipper-correlator is used. Similar behavior is noted in our Class B example here: 25.0 db and 1.3 db, respectively.

When <u>incoherent</u> reception (of coherent signals) is employed, the degradation in $\langle a_o^2 \rangle_{\text{min}}$ is halved (in db) cf. (6.53), viz. -20.8, -1.8 db (Class A), and -12.5 db, -0.7 db (Class B), respectively, again for the same performance and sample sizes.

On the other hand, the more limited ARE's, (Sec. 6.3.3), (III, Sec. 7.4), (6.60), and Table 7.1, show that $(\text{ARE})_{\text{inc}} = (\text{ARE})^2_{\text{coh}} = \Phi^*_{\text{d-coh}}$ (for coherent signal waveforms). For example, in the coherent cases, ARE of clipper-correlator to optimum = $\frac{1}{2}(-3.5) = -1.8$ db, cf. (7.54) in Class A noise, and is -0.7 db in our Class B noise above, cf. (7.55). In contrast, the ARE of the simple correlator is -20.8 db, and -12.5 db, respectively, in Class A and B interference [cf. (7.54),(7.55)]. Of course, the more complete and revealing measures of performance are the error probabilities (P_e^*, P_e) and the probabilities of correct signal detection (p_D^*, p_D) themselves, or the associated minimum detectable signals (which are implicit functions of these probability controls, through B* or B, cf. (7.41), or (6.11b), and Figures 7.5, 7.6.

Other related comparisons may be made the same way. For example, for the same minimum detectable signal and probability control [Case III, Sec. 6.3] we can determine how much longer data acquisition must be for various suboptimum algorithms vis-à-vis the corresponding optimum algorithm (i.e., how much larger sample size n is vs. n*). For our particular example above (coherent detection) we find that:

(i.) Optimum vs. Simple-Correlator:

$$n_{coh} = n^*_{coh}/\Phi^*_d = n^*_{coh} L^{(2)}_{A,B} \quad , \tag{7.56}$$

or

$$n_{coh} = 1.41 \times 10^4 \times n^*_{coh} \quad \text{(Class A)} \ ,$$

and

$$n_{coh} = 3.2 \times 10^2 \times n^*_{coh} \quad \text{(Class B)} \ . \tag{7.56a}$$

Likewise,

(ii.) Optimum vs. Clipper-Correlator:

$$n_{coh} = 2.24 \times n^*_{coh} \quad \text{(Class A)},$$

and

$$n_{coh} = 1.35 \times n^*_{coh} \quad \text{(Class B)}. \tag{7.56b}$$

Again, the simple-correlator is much inferior to the corresponding optimum processor, requiring a much larger sample (or observation time), whereas the clipper-correlator is considerably closer to optimum, requiring only about a factor of two (or less) increase in sample size (n). Similar behavior is encountered in the noncoherent cases, cf. (6.56),(6.57), where we must implement Eqs. (7.31)-(7.38) for specific numerical results.

Many other comparisons between optimum and suboptimum threshold algorithms can be carried out in similar fashion based on the analytic and computational results in this study. We reserve such to a subsequent investigation.

8. SUMMARY OF RESULTS AND CONCLUDING REMARKS:

Here we briefly summarize the principal general results of this study, reminding the reader that the detailed quantitative, analytic results are developed principally in Sections 2 through 7, and in the various Appendices following, as a review of the Table of Contents reveals.

Sections 2 through 4 are mainly an overview of recent earlier work, needed for the subsequent developments of Sections 6 and 7, containing some new material on suboptimum detection algorithms. Section 5 focuses on the structural form of the various optimum threshold detectors, which, like the analytic theory herein described, is canonical; i.e., independent of specific signals and noise. The principal result here is the observation that these threshold algorithms require a double matching process--the earlier, and more familiar linear matched filter for the signal, against a nonlinear transformation of the input noise (and possibly weak signal)--and an initial matching of the receiver to the noise itself: namely, the above-mentioned nonlinear transformation of the (sampled) input data $\underset{\sim}{x}$. The specifics of this transformation dynamics depends, of course, on the pdf of the noise. The overall character of the receiver is adaptive--to the noise, and to the desired signal, as we note more fully below in (11).

Sections 6 and 7, along with the appendices, contain the bulk of the many new results, in particular for incoherent and composite detection. Let us now briefly list the principal general results:

(1) The optimum coherent threshold detector is superior (in the sense of smaller minimum detectable signal, etc.) to the corresponding incoherent detector when the signal waveform is incoherent, as often happens, for instance, when there is a doppler spreading produced in the channel. On the other hand, for coherent signal waveforms, these coherent and incoherent detectors are essentially comparable in threshold detection [cf. Section 6.4, III; Examples 2-5, Section 7.6].

(2) Threshold optimum systems are superior to (threshold) suboptimum systems, as expected. The former can be very much better O(20 db or more) than conventional detectors, optimized against gaussian system noise; e.g., simple correlation detectors. They are less dramatically superior O(2-6 db or so) to clipper-correlation detectors (which employ hard limiters). The

degree of superiority is also greater for Class A noise than it is for the "impulsive" Class B interference (cf. Section 7.6). These results support the use of simple, approximate detector structures, like the clipper-correlation detector, vis-à-vis the exact characteristics (cf. Figures 7.1,7.2a,b) in many instances, because of the much greater complexity of the latter.

(3) We remark that the optimum threshold detectors themselves become suboptimum for input signal levels above some limiting value, where the condition for asymptotic optimality (AO), namely, (approximately) equal variances of the test statistic under H_0 and H_1, is no longer satisfied. It is then not guaranteed that they will remain superior to the aforementioned (or any other) suboptimum detector. However, performance, on an absolute basis, improves for both as the input signal level rises. This means, of course, that even if the AO condition no longer holds, we can still adequately use the originally optimum threshold algorithm.

(4) For these threshold detectors to maintain their optimality for the large data sample sizes ($n>>1$) needed to achieve adequately small decision error probabilities for the very small input signals which are encountered, it is critical that the algorithm include the proper bias term, $\hat{B}_n^*$. This bias is obtained by terminating (under H_0) the basic expansion of the generally optimum likelihood ratio about the null signal ($\theta=0$), cf. Section 2. This bias is solely a function of rms input signal level (a_0^2), sample size (n), the basic noise statistics and second-order signal statistics. In fact, it is shown that $\hat{B}_n^*$ is $-\frac{1}{2}\,\mathrm{var}_0 g_n^* = \frac{1}{2}\left[\left\langle g_n^{*2}\right\rangle_{H_0} - \left\langle g_n^*\right\rangle_{H_0}^2\right] = -\frac{1}{2}\,\sigma_0^{*2}$, cf. Appendix, Section A.3-6. Without this proper bias term (lacking in most analyses of the threshold detection problem [48], performance can be far from optimum [cf. end of Section 6.3].

(5) For best operation, the composite detector is proposed: this is the sum of the coherent and (purely) incoherent algorithms [cf. Section 6.5]. When it is possible to take advantage of the coherent mode as well as the incoherent one, the result is an improvement in performance O(2 db or more) over incoherent reception, and markedly so O(10 db+, η=0.9+) against fading to which (slow or rapid) the coherent detection is particularly vulnerable, as is the incoherent detector to rapid fading, cf. Example 6, Section 7.6. These observations apply generally to both the optimum and suboptimum threshold detectors.

(6) A very important feature of the analysis generally is its canonical character: this is true equally of the statistical-physical noise models employed and of the (optimum) threshold forms of detection algorithm. The formal structure of both algorithm and performance measure is independent of specific physical models. This gives the threshold theory its very considerable breadth: it is possible to indicate the basic functional elements of the algorithms' operations without having to choose a specific physical, numerical example.

(7) Another important feature of the present approach is its definition and use of the concepts of minimum detectable signal and processing gain [cf. Section 6.2 et seq.]. These, in turn, require a nonvanishing input signal, which is certainly the case practically. The AO condition [cf. (3)] is really a condition of small but nonzero input signals, sometimes referred to as "vanishingly small": we call it here "practically small"; i.e., small enough that the AO condition is practically approximated; e.g., $\overset{v}{x}_{max},\overset{v}{y}_{max} = \overset{v}{x}^{*}_{o},\overset{v}{y}^{*}_{o}$ - 15 db, say, so that $\sigma^{*2}_{1} \doteq \sigma^{*2}_{o}$, where $\sigma^{*2}_{1} = \sigma^{*2}_{o} + F(n,\theta)$ and $\therefore |F(n,\theta)| << (\sigma^{*}_{o})^{2}$ or $|F_n|/\sigma^{*2}_{o} << 1$, cf. Sections 6.2, 6.4. The minimum detectable signal and processing gain permit a variety of useful system comparisons, both between optimum detectors in different modes of operation and between optimum and suboptimum receivers.

(8) The concept of Asymptotic Relative Efficiency (ARE), cf. Section 6.3, IV, though useful here, is not a complete nor necessarily reliable measure of system comparisons. A more effective measure is the degradation factor, $\Phi^{*}_{d\text{-coh}}$, $\Phi^{*}_{d\text{-inc}}$, etc., which specifies the increase needed in the minimum detectable signal of suboptimum (threshold) detectors to achieve the same performance as the corresponding optimum detector [cf. Section 7.6, II, also]. Since the minimum detectable signal is an implicit function of the performance probabilities, as well as sample size, noise statistics, etc., it is itself a "complete" performance measure also, while the ARE is not. Error probabilities (and/or probabilities of correct signal detection) are likewise the corresponding "complete" measures of performance, vis-à-vis signal-to-noise ratio, and the ARE, which is of the same level of statistical incompleteness.

(9) The rôle of discrete vis-à-vis continuous sampling is also examined here, in sufficient detail to explain the often "anomalous" behavior of incoherent threshold detectors (for the same P_e^* or p_D^* and sample size, n), giving smaller minimum detectable signals than the corresponding coherent threshold detectors, under discrete sampling, cf. Section 6.4, III. Although these effects are noticeable, they are small O(1-3 db).

(10) Another canonically important feature of the threshold theory is that it provides both structural and performance limits in the optimum cases. Such limits are critical if one is to decide what practical (usually rather suboptimum) systems are to be employed, within the available economy. Often the sacrifice of a few db in $\langle a_o^2 \rangle_{inc}$ is more than compensated for by the resulting simplicity and comparative inexpensiveness of the realization of the algorithms.

(11) In the larger sense, as well as in the particular, these threshold detection algorithms represent adaptive systems: the often very considerable superiority of the optimum algorithms over their various corresponding suboptimum alternatives stems from the fact that the former are basically adaptive. The principal area of adaptivity is the noise. In practice this takes the form of establishing (i), the class of noise--Class A vs. Class B, for example; and (ii), the three (or more) statistical-physical parameters of the particular noise environment of the class in question. Of course, in practice only estimates based on finite samples are possible, so that it is also important to determine how sensitive both the algorithms and their performance are to departures from the actual (infinite-sample) values of the parameters. This involves a robustness study. Preliminary analysis [42],[45] indicates a reasonable lack of sensitivity to small and moderate changes in parameter estimates. A second area of adaptivity lies in the signal domain: estimation of various signal parameters (amplitude, waveform, frequency, etc.) which may only be known statistically at the receiver, or even estimation of such statistics themselves. Some preliminary work employing locally optimum Bayes estimators (LOBE's), which are also AO, is now available [51].

A concise (and incomplete) overview of the material of this report is given in [49]; a much more comprehensive, invited review paper is scheduled [50].

Many further topics need to be studied in the context of the present approach: for example, along the lines of using appropriate estimator-correlators to simplify the realizations of these AO LOBD's, [52], including the proper biases (4) above; and the effects of weakly-dependent noise samples, cf. [53], but along the present lines of "parametric" models, rather than non-parametric ones, [21]-[24]. A parallel derivation for AO LOBE's of specific signal elements, extending the work of [51] in detail, is also needed. Finally (but not necessarily only), is further work along the lines of [54], specifically addressed to multiple-element arrays and beam-forming in nongaussian noise fields. Still other, associated threshold reception problems will suggest themselves in the course of the above, among them the further development of analytical and numerical results for the binary signal cases, which are initiated here.

REFERENCES

[1a]. A.D. Spaulding and D. Middleton, "Optimum Reception in an Impulsive Interference Environment", OT Report 75-67, June, 1975, Office of Telecommunications, U.S. Dep't. of Commerce, NTIS Acces. No. COM75-11097/AS.

[1b]. A.D. Spaulding and D. Middleton, "Optimum Reception in an Impulsive Interference Environment: Part I, Coherent Detection; Part II, Incoherent Reception", IEEE Trans. on Communications Vol. COM-25, Sept., 1977, pp. 910-934. (This is a shortened version of [1a].)

[2]. D. Middleton, "Statistical-Physical Models of Urban Radio-Noise Environments, Part I: Formulations", IEEE Trans. Electromagnetic Compat. Vol. EMC-14, pp. 38-56, May, 1972.

[3]. _____, "Probability Models of Received, Scattered, and Ambient Fields", Proc. IEEE-1972 Int'l. Conf. on Engineering in the Ocean Environment, Newport, R.I., Sept. 13-16, 1972, IEEE Pub. 72-CHO--660-1-OCC, pp. 8-14, "Ocean '72".

[4]. _____, "Statistical-Physical Models of Man-made Radio Noise, Part I: First-order Probability Models of the Instantaneous Amplitude", OT Report 74-36, April, 1974. Office of Telecommunications, U.S. Dep't. of Commerce, NTIS Acces. No. COM75-10864/AS.

[5]. _____, "Statistical-Physical Models of Man-made and Natural Radio Noise, Part II: First-order Probability Models of the Envelope and Phase", OT Report 76-86, April, 1976, Office of Telecommunications, (U.S. Dep't. of Commerce), NTIS Acces. No. PB253949. See [6] below:

[6]. _____, "Statistical-Physical Models of Electromagnetic Interference", IEEE Trans. on Electromagnetic Compatibility, EMC-19, No. 3, pp. 106-127, Aug. 1977. (This is a condensed version of [5].)

[7]. _____, "Procedures for Determining the Parameters of the First-Order Canonical Models of Class A and Class B Electromagnetic Interference", IEEE Trans. on Electromag. Compat. EMC-21, No. 3, pp. 190-208, Aug., 1979.

[8]. _____, "New Results in the Development of Canonical and Quasi-Canonical EMI Probability Models", paper B-1, pp. 25-32, in Proceedings of the 4th Int'l. Symposium on Electromagnetic Compatibility, March 10-12, 1981, Zurich, Switz. (See [9] for a corrected account of Sec. 4.1.)

[9]. _____, "Performance of Telecommunications Systems in the Spectral-Use Environment: VII. Interference Scenarios and the Canonical and Quasi-Canonical (First-Order) Probability Models of Class A Interference", Contractor Report 82-18, March 1982, NTIA, U. S. Dep't. of Commerce, Wash. D.C., NTIS Acces. No. PB82-226861. also, IEEE Trans. on EMC, Vol. 25, May 1983.)

[10]. A.D. Spaulding, "Man-made Noise: The Problem and Recommended Steps toward Solution", OT Report 76-85 (pp. 173), April, 1976, Office of Telecommunications (U.S. Dep't. of Commerce), NTIS Acces. No. PB 253745/AS.

[10a]. (Chemical Rubber Co.,) Handbook of Atmospherics, Ed. by Hans Vollon Vol. II, 1982 (esp. articles by G.H. Hagn); CRC, 2000 N.W. 24th St., Boca Raton, Florida 33431.

[11]. J.H. Van Vleck and D. Middleton, "A Theoretical Comparison of the Visual, Aural, and Meter Reception of Pulsed Signals in the Presence of Noise", J. Appl. Physics, Vol. 17, pp. 940-971, Nov., 1946. (See, in particular, Part I, Sec. II, and p. 944. See, also, D. Middleton, IEEE Communications Soc. Magazine, pp. 9,10, July, 1978.

[12]. D. Middleton, An Introduction to Statistical Communication Theory McGraw-Hill (New York), 1960.

[13]. D. Middleton, "Canonical Non-Gaussian Noise Models: Their Implications for Measurement and for Prediction of Receiver Performance", IEEE Trans. on Electromagnetic Compatibility, EMC-21, No. 3, August 1979, pp. 209-220.

[14]. _____, "Canonically Optimum Threshold Detection", IEEE Trans. on Information Theory, Vol. IT-12, No. 2, April, 1966, pp. 230-243.

[15]. _____, "The Statistical Theory of Detection, I", M.I.T. Lincoln Laboratory Report No. 35, Nov. 1953. See, also, highlights of this Report, published as "Statistical Theory of Detection", Symposium on Statistical Methods in Communication Engineering, IRE Trans. on Info. Theory, PGIT-3, p. 26, March 1954.

[16]. D. Middleton, Ref. [12], Sec. 19.4.

[17]. P. Rudnick, "Likelihood Detection of Small Signals in Stationary Noise", J. Appl. Phys. 32, p. 140, Feb., 1961.

[18]. J. Capon, "On the Asymptotic Efficiency of Locally Optimum Detectors", IRE Trans. on Info. Theory, Vol. IT-7, pp. 67-71, April, 1961.

[19]. D. Middleton and D. Van Meter, "Detection and Extraction of Signals in Noise from the Point of View of Statistical Decision Theory", J. Soc. Industrial and Applied Math., Vol. 3, pp. 192 (1955), Vol. 4, 86 (1956), esp.

[20]. D. Middleton, Topics in Communication Theory, McGraw-Hill (New York), 1965; and RAND Report RM-4687-PR, Nov., 1965. See also the Nirenberg-Middleton Letter to the Editor, IEEE Trans. Comm. Vol. COM-23, p. 1002, Sep't. 1975, for a brief listing of other references.

[21]. J.B. Thomas, "Nonparametric Detection", Proc. IEEE, 58, pp. 623-631, 1970.

[22]. J.H. Miller and J.B. Thomas, "Detectors for Discrete Time Signals in Non-gaussian Noise", IEEE Trans. Info. Theory, Vol. IT-18, pp. 241-250, 1972.

[23]. M. Kanefsky and J.B. Thomas, "On Polarity Detection Schemes with Nongaussian Inputs", J. Franklin Inst., pp. 120-138, 1965.

[24]. S.A. Kassam and J.B. Thomas, "A Class of Nonparametric Detectors for Dependent Input Data", IEEE Trans. Info. Theory, Vol. IT-21, pp. 431-437, 1975. See also Saleem A. Kassam, "A Bibliography on Nonparametric Detection", IEEE Trans. Info. Theory, Vol. IT-26, No. 5, Sept., 1980, for many additional related papers.

[25]. O.Y. Antonov, "Optimum Detection of Signals in Non-Gaussian Noise", Radio Eng. + Electronic Phys., Vol. 12, 541-548, 1967.

[26]. B.R. Levin and A.F. Kushnir, "Asymptotically Optimal Algorithms of Detection and Extraction of Signals from Noise", Radio Eng. and Electron. Phys. Vol. 14, No. 2, pp. 213-221, 1970 (1969 Russian Ed.).

[27]. B.R. Levin and Y.S. Shinakov, "Asymptotic Properties of Bayes Estimates of Parameters of a Signal Masked by Interference", Int'l. Symp. on Info. Theory, Noordwijk, The Netherlands, June 15-19, 1970.

[28]. B.R. Levin, A.F. Kushnir, add A.I. Pinskii, "Asymptotically Optimum Algorithms for Detection and Discrimination of Signals Immersed in Correlated Noise," Rad. Eng. and Electron. Phys., Vol. 14, No. 2, 784-793, 1970 (1969 Russian Ed.).

[29]. J.J. Sheehy, "Optimum Detection of Signals in Nongaussian Noise", J. Acous. Soc. Amer., 63 (1), Jan; 1978, pp. 81-90.

[30]. D. Middleton, "Performance of Telecommunications Systems in the Spectral-Use Environment: Part V: Land-Mobile and Similar Scenarios in Class A Interference". NTIA Contractor Report 79-4, June 1979, NTIA, U.S. Dep't. of Commerce, NTIS Acces. No. PB80-112097.
cf. Sec. 3.

[31]. D. Middleton and D.J. Cohen, "_____: Part VIII. Channel Occupancy Statistics for Land-Mobile and Other Scenarios in Class A Interference", in preparation.

[32]. D. Middleton, "_____; Part VII. Interference Scenarios and the Canonical and Quasi-Canonical (First-Order) Probability Models of Class A Interference," NTIA-CR-82-18, March, 1982 (see [9]).

[33]. A.D. Spaulding, "Optimum Threshold Signal Detection in Broad-Band Impulsive Noise Employing Both Time and Spatial Sampling", IEEE Trans. on Communications, Vol. COM-29, No. 2, February, 1981, pp. 147-152.

[34]. D. Middleton, "Threshold Signal Reception in Electromagnetic Interference Environments: Part II. Receiver Structures and Performance for Class A EMI Environments and Scenarios", NTIA Contractor Report 81-17, March, 1982, for ITS/NTIA, Boulder, Colo. 80303, NTIS Acces. No. PB82-226846.

[35]. R.S. Kennedy, Fading Dispursive Communication Channels, John Wiley (New York), 1969; esp. Chapters 2,3.

[36]. V.V. Ol'shevskii, Statistical Methods in Sonar, Plenum (New York-Consultant's Bureau), 1978, cf. Chapters 4,5.

[37]. D. Middleton, "Channel Characterization and Threshold Reception for Complex Underwater Media", EASCON Sept-Oct.'80, IEEE-0531-6863/80/0000 -171; pp. 171-180, and references.

[38]. _____, "The Underwater Medium as a Generalized Communication Channel", p. 589-612 of Underwater Acoustics and Signal Processing Ed, L. Bjørnø, NATO Advanced Study Institute, D. Reidel Pub. Co., Dordrecht, Holland, 1981.

[39]. B.R. Levin, Theoretical Principles of Statistical Radio Engineering, III, "Soviet Radio", Moscow, 1976, cf. Chapters 1 and 3 in particular

[40]. L. LeCam, "On the Asymptotic Theory of Estimation and Testing Hypotheses", Proc. 3rd Berkeley Symposium on Math. and Statistics, 1956.

[40a]. L. LeCam, "Locally Asymptotically Normal Families of Distributions, Univ. of Cal. Publications in Statistics," U. of Cal. Press, Berkeley, Vol. 3, pp. 37-98, 1960.

[41]. E.L. Ince, Ordinary Differential Equations, Dover, New York, 1944.

[42]. A.D. Spaulding, "Robustness of LOBD's for NonGaussian Noise", pp. 143-152, Proceedings 5th International Symposium on Electromagnetic Compatibility (EMC), Wroclaw, Poland, Sept. 17-19, 1980

[43]. J.E. Evans and A.S. Griffiths,"Design of a Sanguine Noise Processor Based upon World-Wide Extremely Low Frequency (ELF) Recordings", IEEE Trans. Comm. Vol. COM. 22, no. 4, April, 1974, pp. 528-539.

[44]. R.F. Ingram and R. Houle, "Performance of Optimum and Several Suboptimum Receivers for Threshold Detection of Known Signals in Additive White, Non Gaussian Noise", NUSC Tech. Rep't. 6339, Nov. 24, 1980, NUSC, New London, Conn.

[45]. A.D. Spaulding, "Locally Optimum and Suboptimum Detection Performance in Non-Gaussian Noise", Proceedings Int'l. Comm. Conference (ICC), Philadelphia, June, 1982.

[46]. J.H. Van Vleck and D. Middleton, "The Spectrum of Clipped Noise", Proc. IEEE, Vol. 54, No. 1, Jan. 1966, pp. 2-19.

[47]. D. Middleton, "Some Canonical Approaches to the Evaluation of Telecommunication System Performance", NTIA Contractor Report 81-11, June 1981. (U.S. Dept. of Commerce), NTIS Acces. No. PB81-249310.

[48]. D. Middleton and A.D. Spaulding, Correspondence - IEEE Trans. Information Theory, 1983.

[49]. D. Middleton, "Threshold Detection in Nongaussian Interference Environments: Exposition and Interpretation of New Results for EMC Applications," 5th International Symposium on Electromagnetic Compatibility, Zürich, Switzerland, March 8-10, 1983.

[50]. D. Middleton, G. Hagn, and A. D. Spaulding, "Statistical-Physical Models of Nongaussian Electromagnetic Interference Environments and their Predicted Effects on Telecommunications--a Review (tentative title), invited paper for Proc. IEEE, 1984.

[51]. D. Middleton, "Threshold Signal Reception in Electromagnetic Interference Environments: Part III, An Introduction to Canonical Threshold Signal and Parameter Estimation, NTIA Contractor Report 83-21, Jan. 1983, for NTIA/ITS, Boulder, CO 80303, (NTIS Acces. No. not yet available).

[52]. W. A. Gardner, "Structural Characterization of Locally Optimum Detectors in Terms of Locally Optimum Estimators and Correlators," IEEE Trans. on Inf. Theory, Vol. IT-28, No. 6, Nov. 1982, pp. 924-932.

[53]. H. V. Poor, "Signal Detection in the Presence of Weakly Dependent Noise--Part I: Optimum Detection," pp. 735-744; Part II: "Robust Detection," pp. 744-752, IEEE Trans. On Inf. Theory, Vol. IT-28, No. 5, Sept., 1982.

[54]. D. Middleton, "Multiple-Element Threshold Signal Detection of Underwater Acoustic Signals in Nongaussian Interference Environments," Tech. Rept. (NOSC), approximately May, 1983.

GLOSSARY OF PRINCIPAL SYMBOLS

ARE	Asymptotic Relative Efficiency
$A_{A,B}$	overlap indexes
$\hat{A}_{\alpha}$	Class B parameter
A_o	(peak) signal amplitude
a	fading amplitude
$\langle a_o^2 \rangle^*_{min}$, $\langle a_o^2 \rangle_{min}$	minimum detectable signals
a_o, $\overline{a_o}$, $\sqrt{\overline{a_o^2}}$	normalized signal amplitudes
α, α^*	(conditional) probability of false alarm; α, also, a Class B noise parameter, cf. (3.14c)
α_o	λ_o/λ_1 = ratio of radii
$B^{(*)}$	probability control = $(C,C^*)^2$
$B_n, \hat{B}^*_n, B^*_n$	biases
$b_{1\alpha}$	Class B noise parameter
β, β^*	(conditional) probability of false signal detection
${}_mC_n$	binomial coefficient
C, C^*	probability controls
ε	signal epoch
$F_n(\underset{\sim}{x}\|\Theta)$	pdf of (signal and) noise
F_i	detector characteristic

G_B	Class B noise parameter
$G_o(\phi)$	beam pattern
$g(\underset{\sim}{x}), g^*,$	detection algorithms
γ	propagation law (exponent)
Γ'	ratio of intensities of gauss to non-gauss components
H_1, H_0, H_{12}, H_{21}	hypothesis states
$h_M,$	weighting function of matched filter
$\hat{I}_{os}$	source signal intensity
$\overline{I}_N$	average noise intensity
$k, \mathcal{K}$	thresholds
$L^{(2)}, L^{(4)}, L^{(1,2)} L^{(6)}$	(1st-order) statistics of the noise
Λ	likelihood ratio
$l_n^{(*)}$	likelihood ratio
ℓ_i, ℓ_j	transfer characteristic, cf. (4.2a)
λ	distance
λ_0, λ_1	boundaries of source domain
m_{ij}	second-moment function of signal amplitudes
$\mu=p/q$	ratio of a priori problems; also, power law of source distribution, cf. Eq. (3.5).
$n, n_{1,2}, n^*$	number of (independent, time) samples

$\Omega_{2A,2B}$	intensity of nongaussian component (Class A,B) noise
$\Delta\omega_d$	doppler "source"
ω_d	doppler shift
P_D, p_D^*	probability of correct signal detection
P_e, P_e^*	error probabilities
Π, Π^*	processing gains
P	a priori probability
Φ_d^*	degradation factor
ψ	mean noise intensity
ϕ, ϕ_o	phases
$Q_n \hat{Q}_n, \hat{Q}_n^{(21)}$	signal structure factors
q	a priori probability
$\hat{r}_o$	normalizing distance
ρ_s	second-moment function of signals
ρ_{ij}	function of signals at (t_i, t_j)
σ_G^2	gauss intensity
$\sigma^{*2}, \sigma_o^2, \sigma_{on}^2, \hat{\sigma}_o, {}^2\sigma_{01}{}^{*2}$,	variances
sgn x	"sign of"
$S, \overline{S}, \overline{S^T}$	normalized signal waveforms
T	data interval
$(H), \Theta$	error function
Θ^2	signal-to-noise ratio
Θ_i	normal signal waveform parameter

W_n	pdf of noise
$w_1(x)$	pdf of noise
x	normalized data sample
x_o^*	coherent bound
y_o^*	incoherent bound

APPENDICES

Part I Optimal Threshold Detectors

(David Middleton)

APPENDIX A-1

Optimum Threshold Structure and Bias Terms: The "On-Off" Cases:

Here we develop the general LOBD structure, including dependent samples, leading to Eq. (2.9) and its various coherent and incoherent special forms (2.11), (2.12). We focus our attention initially on the "on-off" (H_1 vs. H_0) cases, as the extension to the binary signal situation (H_2 vs. H_1) follows immediately from these results, cf. (2.13) et seq. We consider only the general, and usual, case of additive signals and noise, cf. Sec. A.3-4) ff. however, so that

$$\Lambda_n(\underset{\sim}{x}|\theta) \equiv \mu\langle w_n(\underset{\sim}{x}-\underset{\sim}{\theta})_N\rangle / w_n(x)_N \quad ; \; \mu \equiv p/q; \; \underset{\sim}{x} = [x_i] = [x_i/\sqrt{x_i}] \tag{A.1-1}$$

is the likelihood ratio to be expanded according to the threshold concept described in Sec. 2.2.

A1-1: The General LOBD:

We begin by expanding the numerator in appropriate powers of $\underset{\sim}{\theta} = [a_{oj}s_j]$, cf. (2.9a), through $O(\theta^4)$, to obtain

$$\Lambda_n = \mu\Bigg\{1 - \sum_i^n \langle\theta_i\rangle \frac{\partial w_n}{w_n \partial x_i} + \frac{1}{2!}\sum_{ij}^n \langle\theta_i\theta_j\rangle \frac{1}{w_n} \frac{\partial^2 w_n}{\partial x_i \partial x_j}$$

$$- \frac{1}{3!}\sum_{ijk}^n \langle\theta_i\theta_j\theta_k\rangle \frac{1}{w_n} \frac{\partial^3 w_n}{\partial x_i \partial x_j \partial x_k} + \frac{1}{4!}\sum_{ijk\ell}^n \langle\theta_i\theta_j\theta_k\theta_\ell\rangle \frac{1}{w_n} \frac{\partial^4 w_n}{\partial x_i .. \partial x} \cdots\Bigg\}, \tag{A.1-2}$$

where

$$y_i \equiv \frac{\partial}{\partial x_i} \log w_n = \frac{1}{w_n} \frac{\partial w_n}{\partial x_i} \equiv \frac{w_n^i}{w_n} \quad ;$$

$$\frac{\partial^2 w_n}{w_n \partial x_i \partial x_j} = \frac{w_n^{ij}}{w_n} = \frac{\partial^2 \log w_n}{\partial x_i \partial x_j} + \frac{w_n^i w_n^j}{w_n^2} \equiv z_{ij} + y_i y_j \ , \qquad \text{(A.1-2a)}$$

i.e.

$$z_{ij} \equiv \frac{\partial^2}{\partial x_i \partial x_j} \log w_n, \quad \text{with } \frac{1}{w_n} \frac{\partial^3 w_n}{\partial x_i \partial x_j \partial x_k} \equiv \frac{w_n^{ijk}}{w_n} \ , \text{ etc.,}$$

e.g.

$$\frac{\partial^m w_n}{\partial x_i \ldots \partial x_m} \equiv \frac{w_n^{1,2\ldots m}}{w_n} \quad , \text{ etc.} \qquad \text{(A.1-2b)}$$

Our next step is to expand $\log \Lambda_n$, using (A.1-2) and the relation $\log(1+x) = x - (x^2/2) + (x^3/3) - (x^4/4)\ldots$; $|x|<1$:

$$\log \Lambda_n = \log \mu + \log \left[1 - A^{(1)}_{(i)} + \frac{1}{2!} A^{(2)}_{(ij)} - \frac{1}{3!} A^{(3)}_{(ijk)} + \frac{1}{4!} A^{(4)}_{(ijk\ell)} \ldots\right] \qquad \text{(A.1-3a)}$$

$$= \log \mu + \underbrace{\left[-A^{(1)} + \frac{1}{2!} A^{(2)} - \frac{1}{3!} A^{(3)} + \frac{1}{4!} A^{(4)} \ldots\right]}_{\leq O(\theta^4)}$$

$$\underbrace{- \frac{1}{2} \left[A^{(1)^2} + \frac{1}{2!^2} A^{(2)^2} + \ldots - \frac{2A^{(1)}A^{(2)}}{2!} + \frac{2}{3} A^{(1)}A^{(3)} + \ldots\right]}_{\leq O(\theta^4)}$$

$$\underbrace{+ \frac{1}{3} \left[+A^{(1)^3} + \frac{3A^{(1)^2}A^{(2)}}{2!} + \ldots\right]}_{\leq O(\theta^4)}$$

$$\underbrace{- \frac{1}{4} \left[A^{(1)^4} + \ldots\right]}_{\leq O(\theta^4)} \qquad \text{(A.1-3b)}$$

$$\therefore \log \Lambda_n = \log \mu - A^{(1)} + \frac{1}{2!}[A^{(2)} - A^{(1)2}] - \frac{1}{3!}[A^{(3)} - \frac{3!}{2!} A^{(1)}A^{(2)} + \frac{3!A^{(1)3}}{3}]$$

$$+ \frac{1}{4!}[A^{(4)} - \frac{4!}{2!^3} A^{(2)2} - \frac{4!}{3!} A^{(1)}A^{(3)} + \frac{4!}{2!} A^{(1)2}A^{(2)} - \frac{4!}{4} A^{(1)4}] + \ldots , \tag{A.1-3c}$$

which becomes, more compactly

$$\therefore \log \Lambda_n = \log \mu - \sum_{i}^{n} \langle \theta_i \rangle y_i + \frac{1}{2!} \sum_{ij}^{n} \{\langle \theta_i \theta_j \rangle (y_i y_j + z_{ij}) - \langle \theta_i \rangle \langle \theta_j \rangle y_i y_j\}$$

$$+ \Theta_3 + \Theta_4 + O(\langle \theta^5 \rangle) , \tag{A.1-4}$$

where now, specifically

$$\Theta_3 \equiv - \frac{1}{3!} \sum_{ijk}^{n} \{\langle \theta_i \theta_j \theta_k \rangle \frac{w_n^{ijk}}{w_n} - 3\langle \theta_i \rangle \langle \theta_j \theta_k \rangle y_i (y_j y_k + z_{jk})$$

$$+ 2 y_i y_j y_k \langle \theta_i \rangle \langle \theta_j \rangle \langle \theta_k \rangle\} \tag{A.1-4a}$$

$$\Theta_4 \equiv \frac{1}{4!} \sum_{ijk\ell}^{n} \{\langle \theta_i \theta_j \theta_k \theta_\ell \rangle \frac{w_n^{ijk\ell}}{w_n} - 3\langle \theta_i \theta_j \rangle \langle \theta_k \theta_\ell \rangle (z_{ij} + y_i y_j)(z_{k\ell} + y_k y_\ell)$$

$$- 4\langle \theta_i \rangle y_i \langle \theta_j \theta_k \theta_\ell \rangle \frac{w_n^{jk\ell}}{w_n} + 12\langle \theta_i \rangle \langle \theta_j \rangle y_i y_j \langle \theta_k \theta_\ell \rangle (z_{k\ell} + y_k y_\ell)$$

$$- 6\langle \theta_i \rangle \langle \theta_j \rangle \langle \theta_k \rangle \langle \theta_\ell \rangle y_i y_j y_k y_\ell\} . \tag{A.1-4b}$$

For coherent reception, as explained in Sec. 2.2 above, we retain only those terms in $(\underset{\sim}{x})$ which are $O(\langle \theta \rangle)$ and replace terms $O(\langle \theta^2 \rangle)$ by the resulting average (of $\underset{\sim}{x}$) over H_o, e.g. the LOBD here is now

$$g^*_{coh} = [\log \mu + \frac{1}{2!} \sum_{ij}^{n} \{\langle\theta_i\theta_j\rangle\langle y_i y_j + z_{ij}\rangle_{H_o} - \langle\theta_i\rangle\langle\theta_j\rangle\langle y_i y_j\rangle_{H_o}\}] - \sum_i \langle\theta_i\rangle y_i \quad \text{(A.1-5a)}$$

or

$$= [\log \mu + \frac{1}{2!} \sum_{ij} \{\langle y_i[\langle\theta_i\theta_j\rangle - \langle\theta_i\rangle\langle\theta_j\rangle]y_j\rangle_{H_o} + \langle\theta_i\theta_j\rangle\langle z_{ij}\rangle_{H_o}\}] - \sum_i \langle\theta_i\rangle y_i \ , \quad \text{(A.1-5b)}$$

where the expressions in the square brackets are now the bias term, B^*_{n-c}.

Similarly, for purely incoherent reception, we require $\langle\theta_i\rangle = 0$ and $\langle\theta_i\theta_j\theta_k\rangle = 0$, at least,* for the LOBD, so that $\Theta_3 = 0$, and the LOBD now becomes

$$g^*_{inc} = [\log \mu + \frac{1}{4!}\left\langle \sum_{ijk\ell}^{n} \langle\theta_i\theta_j\theta_k\theta_\ell\rangle \frac{w_n^{(ijk\ell)}}{w_n} - 3[\sum_{ij}\langle\theta_i\theta_j\rangle(y_i y_j + z_{ij})]^2 \right\rangle_{H_o}]$$

$$+ \frac{1}{2!} \sum_{ij}^{n} \langle\theta_i\theta_j\rangle\{y_i y_j + z_{ij}\}, \quad \text{(A.1-6)}$$

where the terms independent of the data $(\underset{\sim}{x})$ constitute the bias, B^*_{n-inc}, here.

To summarize, then, we have the LOBD's for coherent and incoherent detection, respectively

with

$$\boxed{g^*_c = B^*_{n-c} - \sum_i^n \langle\theta_i\rangle y_i = B^*_c - \langle\underset{\sim}{\hat{\theta}}\rangle \underset{\sim}{y} \ , \quad \text{(A.1-7)}}$$

$$\boxed{B^*_{n-c} = \log \mu + \frac{1}{2!}\left\langle \underset{\sim}{\tilde{y}}\,[\underset{\sim}{\rho}_\theta - \langle\underset{\sim}{\hat{\theta}}\rangle\langle\underset{\sim}{\tilde{\theta}}\rangle]\underset{\sim}{y} + \langle\underset{\sim}{\tilde{\theta}}\underset{\sim}{z}_\theta\rangle \right\rangle_{H_o}, \quad \underset{\sim}{\rho}_\theta \equiv \langle\underset{\sim}{\theta}\underset{\sim}{\tilde{\theta}}\rangle = \langle\theta_i\theta_j\rangle, \quad \text{(A.1-7a)}}$$

---

* This second condition, $\langle\theta_i\theta_j\theta_k\rangle = 0$, is certainly satisfied for narrowband signals, $s_i = \sqrt{2}\cos[\omega_o(t_i - \epsilon) - \phi_i]$, when the first condition $\langle\theta_i\rangle = 0$ holds. For broad-band signals, however, we require that $\langle\theta_j\theta_k\theta_\ell\rangle = 0$, as well as $\langle\theta_i\rangle = 0$, for this so-called "purely" incoherent reception.

and

$$g^*_{inc} = B^*_{n\text{-}inc} + \frac{1}{2!}[\underset{\sim}{\tilde{y}}\, \underset{\sim}{\rho}_{\theta}\, \underset{\sim}{y} + \langle \underset{\sim}{\tilde{\theta}} \underset{\sim}{z} \underset{\sim}{\theta} \rangle] \ , \tag{A.1-8}$$

where

$$B^*_{n\text{-}inc} = \log \mu + \frac{1}{4!} \Big\langle \sum_{ijk\ell} \langle \theta_i \theta_j \theta_k \theta_\ell \rangle \frac{w_n^{(ijk\ell)}}{w_n} - 3[\sum_{ij} \langle \theta_i \theta_j \rangle (y_i y_j + z_{ij})]^2 \Big\rangle_{H_0} \ , \tag{A.1-8a}$$

which are the results exhibited in Sec. 2.2 above. Here we have explicitly

$$\underset{\sim}{y} = [y_i] = \frac{\partial}{\partial x_i} \log w_n \ ; \quad \underset{\sim}{z} = [z_{ij}] = [\frac{\partial^2 \log w_n}{\partial x_i \partial x_j}] \ ;$$

$$w_n^{(ijk\ell)} \equiv \frac{\partial^4 w_n}{\partial x_i \partial x_j \partial x_k \partial x_\ell} \ . \tag{A.1-9}$$

The results above hold for dependent or uncorrelated samples, e.g.

$$w_n(\underset{\sim}{x}) \left(\neq \atop = \right) \prod_i^n w(x_i),$$

generally.

A.1-2: Independent Sampling:

When the noise samples are independent(but not necessarily stationary)- the limiting situation of our present analysis- very considerable simplifications

in our general results (A.1-7), (A.1-8) above are possible. Now we have

$$w_n(\underset{\sim}{x})_N \equiv w_n(\underset{\omega}{x}|H_o) = \prod_{i=1}^{n} w_1(x_i|H_o) \tag{A.1-10}$$

so that

$$\left.\begin{aligned} y_i &= \frac{\partial}{\partial x_i}\log w_n \to \frac{\partial \log w_i}{\partial x_i} \equiv \ell_i \ ; \\ z_{ij} &= \frac{\partial^2}{\partial x_i \partial x_j}\log(w_i w_j) = \left[\frac{\partial^2}{\partial x_i^2}\log w_i\right]\delta_{ij} = \ell_i'\delta_{ij} \ ; \\ \therefore \left(\frac{w_1''}{w_1}\right)_i &= \frac{\partial^2}{\partial x_i^2}\log w_{1i} + \left(\frac{w_1'}{w_1}\right)_i^2 = \ell_i'\delta_{ij} + \ell_i^2 \ ; \\ \therefore \frac{w_1^{(ij)}}{w_{1i}w_{1j}} &= y_i y_j + z_{ij} = \ell_i\ell_j + \ell_i'\delta_{ij} \ . \end{aligned}\right\} \tag{A.1-11}$$

Accordingly, the LOBD's (A.1-7), (A.1-8) become now

$$\boxed{g_c^* = B_{n\text{-}c}^* - \sum_{i}^{n} \ell_i\langle\theta_i\rangle \ ; \ g_{inc}^* = B_{n\text{-}inc}^* + \frac{1}{2!}\sum_{ij}^{n}[\ell_i\ell_j + \ell_i'\delta_{ij}]\langle\theta_i\theta_j\rangle} \ , \tag{A.1-12}$$

cf. (4.1), (4.2), (4.4).

Our next task here is to obtain the biases (A.1-7a), (A.1-8a), for these independent samples. We begin with <u>the coherent case</u> (A.1-7a) and observe that

$$\sum_{ij} a_{ij}\langle y_i y_j\rangle_{H_o} = \sum_{i} a_{ii}\langle y_i^2\rangle_{H_o} + \sum_{ij}{}' a_{ij}\langle y_i\rangle_{H_o}\langle y_j\rangle_{H_o} , \tag{A.1-13a}$$

since x_i, x_j $(i \neq j)$ are independent, so that

$$\sum_{ij} a_{ij} \langle y_i y_j \rangle_{H_o} = \sum_i a_{ii} \langle y_i^2 \rangle_{H_o}$$

$$\langle y_i \rangle_{H_o} = \int_{-\infty}^{\infty} \ell_i w_{1i} dx_i = \int_{-\infty}^{\infty} w'_{1i} dx_i = w_{1i} \Big|_{-\infty}^{\infty} = 0 \ , \qquad \text{(A.1-13b)}$$

(regardless of whether or not w_1 is symmetrical!). This last follows from the necessary condition on the proper pdf w_{1i} that $w_1(\pm\infty)_i = 0$ always. Similarly, we have

$$\sum_{ij} b_{ij} \langle z_{ij} \rangle_{H_o} = \sum_{ij} \langle \theta_i \theta_j \rangle \langle \ell'_i \delta_{ij} \rangle_{H_o} = \sum_i \langle \theta_i^2 \rangle \int_{-\infty}^{\infty} \ell'_i w_{1i} dx_i$$

$$= \sum_i \langle \theta_i^2 \rangle \left(\int_{-\infty}^{\infty} \left[\frac{w''_1}{w_1} - \left(\frac{w'_1}{w_1} \right)^2 \right] w_1 dx \right)_i$$

$$= - \sum_i \langle \theta_i^2 \rangle \left(\int_{-\infty}^{\infty} \left(\frac{w'_1}{w_1} \right)^2 w_1 dx \right)_i \quad ; \quad \int_{-\infty}^{\infty} w''_1 dx_i = w'_1 \Big|_{-\infty}^{\infty} = 0, \qquad \text{(A.1-14)}$$

since $w'_1(\pm\infty) = 0$, also, for a proper pdf. Writing*

$$\boxed{L_i^{(2)} \equiv \int_{-\infty}^{\infty} \left(\frac{w'_1}{w_1} \right)_i^2 w_{1i} dx_i = \langle \ell_i^2 \rangle_{H_o}} = \langle y_i^2 \rangle_{H_o} \ , \qquad \text{(A.1-15)}$$

and observing that $a_{ii} = \rho_\theta|_{ii} - \langle \theta_i \rangle^2 = \langle \theta_i^2 \rangle - \langle \theta_i \rangle^2$; $b_{ii} = \langle \theta_i^2 \rangle$ in the above, we find that the bias (A.1-7a) becomes

---

*Incidentally, note that $L_i^{(2)}$ is equivalent to Fisher's Information I_i, at $\theta=0$, cf. Eq. (225),[12], i.e.,

$$I_i \Big|_{\theta-0} = \left\{ \left(\left[\frac{\partial / n \ w_1(x_i - \theta_i)}{\partial \theta_i} \right]^2 w_i(x_i | \theta_i) dx_i \right\}_{\theta=0} \right.$$

$$B^*_{n\text{-coh}} = \log \mu - \frac{1}{2}\sum_i^n \langle \theta_i \rangle^2 L_i^{(2)} = \log \mu + \hat{B}^*_{n\text{-coh}} \,. \qquad \text{(A.1-16)}$$

When the noise process $\{\underset{\sim}{x}\}$ is stationary, $w_{1i} = w_1$, all i and $\therefore\ \psi_i = \psi$, $L_i^{(2)} = L^{(2)}$, all i, etc., further considerable simplification occurs. We obtain for the coherent LOBD, g^*_{coh}, from (A.1-7), (A.1-16), $\ell_i = \ell_i(x_i) \to \ell(x_i)$ and

$$\therefore \quad g^*_{coh} = [\log \mu - L^{(2)} \sum_{i=1}^n \tfrac{1}{2}\langle a_{oi} s_i \rangle^2] - \sum_{i=1}^n \langle a_{oi} s_i \rangle \ell(x_i). \qquad \text{(A.1-17)}$$

Our next task is to evaluate the bias, (A.1-8a), for incoherent detection, now with independent sampling. Let us consider the first term of (A.1-8a), viz.

$$\left\langle \sum_{ijk\ell} \langle \theta_i \theta_j \theta_k \theta_\ell \rangle \frac{w_n^{(ijk\ell)}}{w_n} \right\rangle_{H_o} :$$

I. $(i \neq j \neq k \neq \ell)$:

$$\therefore \left\langle \frac{w_n^{(ijk\ell)}}{w_n} \right\rangle_{H_o} = \left\langle \frac{w_1^{(i)}}{w_{1i}} \cdot \frac{w_1^{(j)}}{w_{ij}} \cdot \frac{w_1^{(k)}}{w_{ik}} \cdot \frac{w_1^{(\ell)}}{w_i} \right\rangle_{H_o} = \langle \ell_i \rangle_o \langle \ell_j \rangle_o \langle \ell_k \rangle_o \langle \ell_\ell \rangle_o = 0,$$

cf. (A.1-13b) ; (A.1-18a)

II. $i=j(\neq k \neq \ell)$:

$$\left\langle \frac{w_n^{(ijk\ell)}}{w_n} \right\rangle_{H_o} = \left\langle \frac{w_1^{(ii)}}{w_{1i}} \cdot \frac{w_1^{(k)}}{w_{1k}} \cdot \frac{w_1^{(\ell)}}{w_1} \right\rangle_{H_o} = \left\langle \left(\frac{w_1''}{w_1}\right) \right\rangle_{H_o} \langle \ell_k \rangle_o \langle \ell_\ell \rangle_o = 0,$$

cf. (a.1-13b) ; (A.1-18b)

There are ${}_{N}C_{N-(E-1)}$ combinations of the above, where N = no. of indexes (= 4 here) and E no. of indexes that are equal, i.e. k=j, ∴ E = 2, so that ${}_{4}C_{4-1} = {}_{4}C_{3} = 4$ combinations of the above. (For I, E = 1 (identity), ∴ ${}_{4}C_{4-0} = 1$.)

III. i=j; k=ℓ (i≠k):

$$\left\langle \frac{w_n^{(ijk\ell)}}{w_n} \right\rangle_{H_o} = \left\langle \frac{w_1^{(ii)}}{w_{1i}} \right\rangle_o \left\langle \frac{w_1^{(kk)}}{w_{1k}} \right\rangle_o = \left\langle \left(\frac{w_1''}{w_1}\right)_i \right\rangle_o \left\langle \left(\frac{w_1''}{w_1}\right)_k \right\rangle_o = \langle \ell_i^2 \delta_{ij} + \ell_{ij}^2 \rangle_o \langle \ell_k^2 \delta_{k\ell} + \ell_{k\ell}^2 \rangle_o = 0$$

cf. (A.1-11), (A.1-14). (A.1-18c)

Similarly, we have

IV. i = j = k(≠ℓ):

$$\left\langle \frac{w_n^{(ijk\ell)}}{w_n} \right\rangle_{H_o} = \left\langle \frac{w_1^{(iii)}}{w_{1i}} \right\rangle_o \left\langle \frac{w_1^{(\ell)}}{w_{1\ell}} \right\rangle_o = 0, \text{ since } \left\langle \frac{w_1^{(\ell)}}{w_{1\ell}} \right\rangle_o = \left\langle \left(\frac{w_1'}{w_1}\right)_\ell \right\rangle_o = \langle \ell \rangle_{\ell,o} = 0$$

(A.1-18d)

V. (i=j=k=ℓ):

$$\left\langle \frac{w_n^{(ijk\ell)}}{w_n} \right\rangle_{H_o} = \left\langle \left(\frac{w_1^{(4)}}{w_1}\right)_i \right\rangle_o = 0, \text{ since } \left(\int_{-\infty}^{\infty} w_1^{(4)} dx\right)_i = w_{1i}^{(3)} \Big|_{-\infty}^{\infty} = 0. \quad \text{(A.1-18e)}$$

Accordingly, the first term of (A.1-8a), (apart from log μ) vanishes.

The second term, however, has a definite, nonzero contribution. We distinguish the following combinations of terms, on expanding:

$$-\frac{1}{8}\left\langle\left[\sum_i\langle\theta_i^2\rangle\frac{w_{1i}^{(")}}{w_{1i}}+\sum_{ij}^{(i\neq j)}\langle\theta_i\theta_j\rangle\ell_i\ell_j\right]\left[\sum_k\langle\theta_k^2\rangle\frac{w_{1k}^{(")}}{w_{1k}}+\sum_{k\ell}^{(k\neq\ell)}\langle\theta_k\theta_\ell\rangle\ell_k\ell_\ell\right]\right\rangle_{H_o}:$$

(A.1-19)

(1). (i≠k):

$$\left\langle w_{1i}^{(")}/w_{1k}\right\rangle_o=\left\langle\frac{w_{1i}^{(")}}{w_{1k}}\right\rangle_o\left\langle\frac{w_{1k}^{(")}}{w_{1k}}\right\rangle_o=0\ :\qquad\text{(A.1-19a)}$$

(2). (i=k):

$$\boxed{\left\langle\left(\frac{w_{1k}^{(")}}{w_{1i}}\right)^2\right\rangle_o=\left(\int_{-\infty}^{\infty}\left(\frac{w_1''}{w_1}\right)^2w_1\,dx\right)_i\equiv L_i^{(4)}\ (>0),=\left\langle(\ell_i'\delta_{ij}+\ell_i^2)^2\right\rangle_{H_o},}$$

cf. (A.1-18c); (A.1-19b)

(3). (i≠j)≠(k≠ℓ):

$$\langle\ell_i\ell_j\ell_k\ell_\ell\rangle_o=\langle\ell_i\rangle_o\langle\ell_j\rangle_o\langle\ell_k\rangle_o\langle\ell_\ell\rangle_o=0;\qquad\text{(A.1-19c)}$$

(4). (i≠j); (k≠ℓ):

$$\left.\begin{matrix}\text{(a).}\ \ i=k\\(j\neq\ell)\end{matrix}\right\}:\ \langle\ell_i^2\ell_j\ell_\ell\rangle_o=0\ ;\qquad\text{(A.1-19d)}$$

$$\text{(b).}\left\{\begin{matrix}i=k;\ j=\ell\\ \\ i=\ell;\ j=k\end{matrix}\right\}(k\neq\ell)\ (i\neq j)\ ;\quad\begin{matrix}\langle\ell_i^2\ell_j^2\rangle_o=\langle\ell_i^2\rangle_o\langle\ell_j^2\rangle_o=L_i^{(2)}L_j^{(2)}\ ,\\ \langle\ell_i^2\ell_k^2\rangle_o=\langle\ell_i^2\rangle_o\langle\ell_k^2\rangle_o=L_i^{(2)}L_k^{(2)}\ .\end{matrix}\qquad\text{(A.19c)}$$

Combining (A.1-19a-e) we get for (A.1-19), and in fact, for the entire bias term, finally,

$$B^*_{n\text{-inc}} = \log\mu - \frac{1}{8}\{\sum_i^n L_i^{(4)}\langle\theta_i^2\rangle^2 - 2L_i^{(2)^2}\langle\theta_i^2\rangle^2 + 2\sum_{ij} L_i^{(2)}L_j^{(2)}\langle\theta_i\theta_j\rangle^2\}$$

$$\equiv \log\mu + \hat{B}^*_{n\text{-inc}}\ , \qquad \text{(A.1-20a)}$$

and when the noise process is stationary, e.g. $L_i^{(4)} = L^{(4)}$, $L_i^{(2)} = L^{(2)}$, etc. the simpler result

$$\therefore\quad B^*_{n\text{-inc}} = \log\mu - \frac{1}{8}\sum_{ij}\langle\theta_i\theta_j\rangle^2\{(L^{(4)} - 2L^{(2)^2})\delta_{ij} + 2L^{(2)^2}\} \equiv \log\mu + \hat{B}^*_{n\text{-inc}}\cdot \qquad \text{(A.1-20b)}$$

Accordingly, in the stationary cases the incoherent LOBD (A.1-8) now becomes explicitly

$$g^*_{inc} = [\log\mu - \frac{1}{8}\sum_{ij}\langle a_{oi}a_{oj}s_is_j\rangle^2\{(L^{(4)} - 2L^{(2)^2})\delta_{ij} + 2L^{(2)^2}\}]$$

$$+ \frac{1}{2!}\sum_{ij}(\ell_i\ell_j + \ell'_i\delta_{ij})\langle a_{oi}a_{oj}s_is_j\rangle\ , \qquad \text{(A.1-21)}$$

$$\ell_i = \ell(x_i) \qquad = \frac{d}{dx}\log w_1(x|H_o)\Big|_{x=x_i}\ , \text{ etc.,}$$

where the term [ ] $(=B^*_{n\text{-inc}})$ is the bias and $L^{(2)} = \langle\ell^2\rangle_o$; $L^{(4)} = \langle(\ell' + \ell^2)^2\rangle$. cf. (A.1-15), (A.1-19b).

A.1-3: Gauss Noise and Independent Sampling:

Our results (A.1-17), (A.1-21) for g* should reduce to the previously obtained forms when the noise is gaussian. Here we have (for independent noise samples)